Comparisons of the NGA-Subduction ground motion models

Nick Gregor, M.EERI[1] (iD), Kofi Addo, M.EERI[2], Norman A Abrahamson, M.EERI[3], Linda Al Atik[4], Gail M Atkinson, M.EERI[5], David M Boore[6], Yousef Bozorgnia, M.EERI[7], Kenneth W Campbell, M.EERI[8], Brian S-J Chiou[9], Zeynep Gülerce[10] (iD), Behzad Hassani[2], Tadahiro Kishida, M.EERI[11], Nico Kuehn[7], Silvia Mazzoni, M.EERI[7], Saburoh Midorikawa[12], Grace A Parker, M.EERI[6] (iD), Hongjun Si, M.EERI[13] (iD), Jonathan P Stewart, M.EERI[7] (iD), and Robert R Youngs, M.EERI[14]

Abstract

In this article, ground-motion models (GMMs) for subduction earthquakes recently developed as part of the Next Generation Attenuation-Subduction (NGA-Sub) project are compared. The four models presented in this comparison study are documented in their respective articles submitted along with this article. Each of these four models is based on the analysis of the large NGA-Sub database. Three of the four current models are developed for a global version as well as separate regionalized models. The fourth model was developed based on earthquakes only from Japan, and as such is applicable only for Japan. As part of this comparison study, a general discussion on the parameterization of the four models and the regionalization of

[1]Nicholas Gregor Consulting, Oakland, CA, USA
[2]BC Hydro, Burnaby, BC, Canada
[3]University of California, Berkeley, Berkeley, CA, USA
[4]Linda Al Atik Consulting, San Francisco, CA, USA
[5]Western University, London, ON, Canada
[6]United States Geological Survey, Moffett Field, CA, USA
[7]University of California, Los Angeles, Los Angeles, CA, USA
[8]Kenneth W Campbell Consulting, Beaverton, OR, USA
[9]California Department of Transportation, Sacramento, CA, USA
[10]Middle East Technical University, Ankara, Turkey
[11]Khalifa University of Science and Technology, Abu Dhabi, United Arab Emirates
[12]Tokyo Institute of Technology, Tokyo, Japan
[13]Seismological Research Institute Inc., Tokyo, Japan
[14]Wood, Oakland, CA, USA

Corresponding author:
Nick Gregor, Nicholas Gregor Consulting, 32 Camellia Place, Oakland, CA 94602, USA.
Email: nick@ngregor.com

the three models is provided. The specific strengths and or weaknesses or the technical decisions and justifications of any one model are not part of this comparison. A selected suite of deterministic attenuation curves and spectra are presented for the models along with a selected suite of currently used subduction models. A limited number of comparisons are presented in this article with a larger number of comparisons and the digital values provided in the electronic attachment. In addition to these scenario calculation comparisons, the results from a standard probabilistic seismic hazard analysis (PSHA) for two sites located in the Pacific Northwest Region in the state of Washington are presented. These calculations highlight the potential impact of using the new GMMs. Based on the comparisons presented here, a general understanding of these new GMMs can be obtained with the expectation that the implementation of a specific seismic hazard study should incorporate similar and additional comparisons and sensitivity studies pertinent to the site of interest.

Introduction

Following the success of the previous Next Generation Attenuation (NGA) programs, the NGA-Subduction (NGA-Sub) program (Bozorgnia et al., 2021) compiled a large ground motion database (Ahdi et al., 2020, 2021; Bozorgnia and Stewart, 2020; Contreras et al., 2020, 2021; Kishida et al., 2020; Mazzoni et al., 2021) and developed new semi-empirically based ground motion models (GMMs) for subduction earthquakes. Currently, four GMMs have been developed and are presented and compared in this article:

- Abrahamson, N. and Gülerce, Z.   [AG]
- Kuehn, N., Bozorgnia, Y., Campbell, K. and Gregor, N.   [KBCG]
- Parker, G., Stewart, J., Boore, D., Atkinson, G., and Hassani, B. [PSBAH]
- Si, H., Midorikawa, S., and Kishida, T.   [SMK]

The development and more extensive presentation of each of the GMMs are provided in the individual citations from each developer team (Abrahamson and Gülerce, 2020, 2021; Kuehn et al., 2020, 2021; Parker et al., 2020, 2021; Si et al., 2020). As such, this article will focus on the comparison of the results between the models and not discuss the technical decisions and choices used by the individual developer teams for the development of each model. For those decisions, the reader is referred to the individual publications for each model. The acronyms provided in the brackets are used throughout this article in the comparison plots to identify the models. Note that the PSBAH model for magnitude scaling for interface events was adjusted between the two publications: Parker et al. (2020, 2021). The comparisons presented in this article are based on the adjusted Parker et al. (2021) version of their model. Extensive comparisons, including the digital files with the earlier model in Parker et al. (2020) model and without the AG model but including the KBCG and SMK models, are presented in a separate report (Gregor et al., 2020).

One feature common to three of the four GMMs (AG, KBCG, and PSBAH) is the development of both a global version and specific regionalized versions of their models. As stated earlier, the SMK model was developed based solely on Japanese data and, as such, should be considered a regionalized model for Japan.

The comparisons will focus on specific aspects of the GMMs given a selected number of commonly encountered control scenario cases in seismic hazard analyses, especially for sites located in the Pacific Northwest. It is recommended that prior to implementing and using these new NGA-Sub GMMs for a seismic hazard study, a relative comparison and an assessment of their predictive features should be performed by the user with their site of interest in mind, in addition to the comparisons presented in this article. Note that only a few of these comparisons are presented in the article but additional comparisons are contained in the digital files associated with the electronic supplement as described in Supplemental Appendix A. All of the input parameters needed for the comparisons presented in this article and the additional comparisons provided in Supplemental Appendix A are contained in the electronic files.

These new NGA-Sub GMMs will also be compared to currently published and commonly used subduction GMMs. This comparison of the new NGA-Sub models with current models is not meant to be a complete comparison of all currently available subduction models. Rather, it is a comparison with those models that have been considered in the U.S. Geological Survey (USGS) National Seismic Hazard Map (Petersen et al., 2014, 2020) and are commonly used in seismic hazard studies for subduction sources both in the United States and internationally. More information about other models not selected for the comparison can be reviewed from the global database of GMMs maintained by J. Douglas (http://www.gmpe.org.uk). In addition to the comparisons of median ground motion estimates, a summary comparison of the aleatory sigma models is presented.

Given the importance of these new GMMs for application to the Pacific Northwest region, an example PSHA calculation is performed for two representative sites based on their relative contribution from deep slab events and the Cascadia interface source in the region. The USGS (Petersen et al., 2014) seismic-source model is used for the PSHA, and sensitivity calculations are presented based on the previously published GMMs and the newly developed GMMs. These results illustrate the differences in the median predictions as well as the differences in the aleatory sigma models from the different GMMs.

Data selection and model applicability range

The NGA-Sub database contains uniformly processed empirical data from seven defined subduction tectonic regions: Alaska, Central America, and Mexico, Cascadia, Japan, New Zealand, South America and Taiwan (Bozorgnia and Stewart, 2020). This empirical database represents the largest and most complete database of subduction ground motions and associated metadata information to date. Given the large NGA-Sub database (Bozorgnia and Stewart, 2020), each modeler team parsed the dataset to select the acceptable data for the GMM development. As noted earlier, the AG, KBCG, and PSBAH teams considered data from all regions, whereas the SMK team only considered data from Japan. Based on the team-specific selection criteria, approximately 10% of the NGA-Sub database is selected as being acceptable and used in the regression analysis for each team. This removal of a large percentage of the NGA-Sub database (i.e. approximately 90%), for example, is based on the limited metadata for a given event and recordings, events classified as non-interface or slab events, recordings classified with poor quality flags, and or anomalous

events. The SMK team had a lower percentage given their restriction to data only from Japan. Based on the team selections, the majority of the acceptable data is from Japan and Taiwan, and a very limited amount of data is available from the Pacific Northwest region, especially for interface events. The reader is referred to the individual citations from each team for the specific selection criteria.

Each of the four GMMs has defined ranges of applicability in terms of moment magnitude (M), closest distance to the rupture surface (R_{RUP}), source depth (either depth to the top of the rupture plane, Z_{TOR}, or hypocentral depth, Z_{HYP}), and the time-averaged shear wave velocity in the top 30 m of the site (V_{S30}). These are summarized in Table 1. The use of any of the models outside of these defined applicability ranges should be performed with caution and—at a minimum—analyses for the behavior of the models should be performed prior to the application of these models outside of their recommended applicable range. These ranges are applicable to the global and regionalized versions of the models except as were indicated in Table 1. All of the GMMs are defined for a full spectral period range of PGA, T = 0.01 sec to 10 s, and PGV.

Model functional forms and parameters

Each modeling team presents their full model functional form in their specific citations (Abrahamson and Gülerce, 2020, 2021; Kuehn et al., 2020, 2021; Parker et al., 2020, 2021; Si et al., 2020). For the AG, KBCG, and PSBAH models that have both global and regional versions, the functional forms of the models are the same with the regionalization being based on regional coefficients for the model constant, linear site amplification, anelastic attenuation, and site response terms. For the three models with regionalized versions, the PSBAH model did not develop a model for New Zealand and recommends the global version of the models for use there. The other regions (Alaska, Cascadia, Central America/Mexico, Japan, South America, and Taiwan) are common to the three GMMs with regional variations. Several input parameters are common to the suite of GMMs, and the full sets of parameters are listed in Table 2 for each of the four GMMs.

A common feature for each model is a magnitude-scaling breakpoint defined separately for interface and slab events. These magnitude-scaling breakpoints are based on either numerical simulations (i.e. AG for interface events from Atkinson and Macias, 2009; Gregor et al., 2002), Japanese data (i.e. SMK model), or the studies by Ji and Archuleta (2018) for slab events and Campbell (2020) for interface events that provide subduction-zone-specific values (KCBG and PSBAH models). Note that for the AG interface model, the period-dependent magnitude-scaling value is based on the BC Hydro model (Abrahamson et al., 2016) and is not regionalized. This magnitude-scaling breakpoint varies from 8.2 for short periods to 7.8 for longer spectral periods. The recommended regionalized magnitude-scaling breakpoints for the models are listed in Table 3.

Basin amplification effects are included in the GMMs using the station metadata for sites located in Japan, Cascadia, New Zealand, and Taiwan. For Cascadia, all three applicable models (i.e. AG, KBCG, and PSBAH) define the basin response as a function of the depth to the 2.5 km/sec shear-wave velocity horizon, $Z_{2.5}$. In addition, a further refinement is modeled for sites located within the Seattle basin and other basins in the Pacific Northwest. For Japan, all four applicable models characterize the basin response based on $Z_{2.5}$. For the KBCG model, two additional basin response models are provided for New Zealand and Taiwan, and these are based on the depth to the 1.0 km/sec shear-wave

Table 1. Model applicability of the NGA-Sub GMMs for magnitude, distance, and V_{S30}

	AG	KBCG	PSBAH	SMK
Magnitude	$6 \leqslant M \leqslant 9.5$ (interface) $5 \leqslant M \leqslant 8.0$ (slab)[a]	$5 \leqslant M \leqslant 9.5$ (interface) $5 \leqslant M \leqslant 8.5$ (slab)	$4.5 \leqslant M \leqslant 9.5$ (interface) $4.5 \leqslant M \leqslant 8.5$ (slab)	$5.5 \leqslant M \leqslant 9.1$ (interface) $5.6 \leqslant M \leqslant 8.3$ (slab)
Distance (km)	$R_{RUP} \leqslant 500$ $R_{RUP} \leqslant 800$[a]	$10 \leqslant R_{RUP} \leqslant 1000$	$20 \leqslant R_{RUP} \leqslant 1000$ (interface) $35 \leqslant R_{RUP} \leqslant 1000$ (slab)	$14 \leqslant R_{RUP} \leqslant 300$ (interface) $18 \leqslant R_{RUP} \leqslant 300$ (slab)
V_{S30} (m/sec)	$150 \leqslant V_{S30} \leqslant 1,500$	$150 \leqslant V_{S30} \leqslant 1,500$	$150 \leqslant V_{S30} \leqslant 2,000$	$100 \leqslant V_{S30} \leqslant 1,900$
Source depth (km)	$Z_{TOR} \leqslant 200$ (slab)[b]	$Z_{TOR} \leqslant 50$ (interface) $Z_{TOR} \leqslant 200$ (slab)[c]	$Z_{HYP} \leqslant 40$ (interface) $20 \leqslant Z_{HYP} \leqslant 200$ (slab)	$4 \leqslant D \leqslant 50$ (interface) $18 \leqslant D \leqslant 100$ (slab)
Region	Global and regional	Global and regional	Global and regional	Japan

AG: Abrahamson and Gülerce (2021); KBCG: Kuehn et al. (2021); PSBAH: Parker et al. (2021); SMK: Si et al. (2020); R_{RUP}: closest distance to the rupture surface; Z_{TOR}: either depth to the top of the rupture plane; Z_{HYP}: hypocentral depth.

[a]For Cascadia events.
[b]Slab depth scaling is constant for $Z_{TOR} > 200$ km.
[c]For Columbia region, $Z_{TOR} \leqslant 150$ km for slab events.

Table 2. Model parameters used for the NGA-Sub GMMs

Parameter	AG	KBCG	PSBAH	SMK
Moment magnitude	**M**	**M**	**M**	**M**
Closest distance to rupture plane (km)	R_{rup}	R_{rup}	R_{rup}	R_{rup}
Depth to top of rupture (km)	Z_{TOR} (slab only)	Z_{TOR}	–	–
Hypocentral depth (km)	–	–	Z_{HYP} (slab only)	D
Moho depth (km)	–	–	–	Moho depth
Average shear-wave velocity in top 30 m (m/sec)	V_{S30}	V_{S30}	V_{S30}	V_{S30}
Depth to 2.5 km/sec boundary (km)	$Z_{2.5}$ (only for Cascadia and Japan Basins)	$Z_{2.5}$ (only for Cascadia and Japan Basins)	$Z_{2.5}$ (only for Cascadia and Japan Basins)	$Z_{2.5}$ (only for Japan Basins)
Depth to 1.0 km/sec boundary (km)	–	$Z_{1.0}$ (only for Taiwan and New Zealand Basins)	–	–
Interface/slab classification	0 = interface 1 = slab	0 = interface 1 = slab	0 = interface 1 = slab	0 = interface 1 = slab
Magnitude-scaling breakpoint	(see Table 3)	(see Table 3)	(see Table 3)	8.3

AG: Abrahamson and Gülerce (2021); KBCG: Kuehn et al. (2021); PSBAH: Parker et al. (2021); SMK: Si et al. (2020); R_{rup}: closest distance to the rupture surface; Z_{TOR}: depth to the top of the rupture plane; Z_{HYP}: hypocentral depth.

Table 3. Regionalized models and magnitude-scaling breakpoint values

Region	AG (Interface/Slab)	KBCG (Interface/Slab)	PSBAH (Interface/Slab)	SMK (Interface/Slab)
Global	8.2-7.8/7.4	7.9/7.6	7.9/7.6	–
Alaska	8.2-7.8/7.9	8.6/7.2	8.6/7.2	–
Alaska—Aleutian	8.2-7.8/7.9	8.0/8.0	8.0/7.98	–
Cascadia	8.2-7.8/7.1	8.0/7.2	7.7/7.2	–
Central America and Mexico—North	8.2-7.8/7.4	7.4/7.4	7.4/7.4	–
Central America and Mexico—South	8.2-7.8/7.4	7.5/7.6	7.4/7.6	–
Japan—Pacific Plate	8.2-7.8/7.6	8.5/7.6	8.5/7.65	8.3/8.3
Japan—Philippine Plate	8.2-7.8/7.6	7.7/7.6	7.7/7.55	8.3/8.3
Northern South America	8.2-7.8/7.5	8.5/7.3	8.5/7.3	–
Southern South America	8.2-7.8/7.5	8.6/7.2	8.6/7.25	–
Taiwan	8.2-7.8/7.7	7.1/7.7	7.1/7.7	–
New Zealand	8.2-7.8/8.0	8.3/7.6	–	–

AG: Abrahamson and Gülerce (2021); KBCG: Kuehn et al. (2021); PSBAH: Parker et al. (2021); SMK: Si et al. (2020).

velocity horizon, $Z_{1.0}$. Regionalized estimation of the predicted $Z_{2.5}$ and $Z_{1.0}$ values as a function of V_{S30} values is provided in the cited references from each of the developer teams.

Median value comparisons

Median ground motion value comparisons are presented for scaling with distance, magnitude, depth to the top of the rupture, and basin amplification. The comparisons are separated based on interface and slab events, except for the basin amplifications, because the basin effects are modeled as independent of the event type. For both the attenuation curves and the response spectra, comparison plots are presented for two V_{S30} values of 760 m/sec and 400 m/sec. The first value is representative of the common reference condition corresponding to the NEHRP B/C boundary site condition. The second and lower value is more consistent with very dense soil and or soft-rock site conditions (American Society of Civil Engineers (ASCE) 2017) and is selected to compare the models for a more generic site condition.

For the global comparisons, the following published models are presented:

- Atkinson and Boore (2003, 2008) [AB08]
- Atkinson and Macias (2009) [AM09]
- Zhao et al. (2006) [Zea06]
- Zhao et al. (2016a, 2016b) [Zea16]
- BC Hydro (Abrahamson et al., 2016) [BCH]
- BC Hydro Update for the USGS (Abrahamson et al., 2018) [BCHU]

Note that these previous ground motion models are defined for the geomean horizontal component, whereas the NGA-Sub GMMs are defined for the RotD50 horizontal component (Bozorgnia and Stewart, 2020; Mazzoni et al., 2021). For all of the comparisons, no spectral period dependent scaling (e.g. Boore and Kishida, 2017) is applied to adjust the geomean horizontal component to the RotD50 component since the comparisons are presented to provide a general comparison between the previous and current GMMs.

The AM09 model is defined specifically for a V_{S30} of 760 m/sec and is only compared for this V_{S30} case. For the AB08 model, the site conditions are defined based on NEHRP categories (Building Seismic Safety Council, 2009), and for the V_{S30} of 760 m/s, the average of NEHRP B and C site conditions ground motions are computed. For the lower V_{S30} value of 400 m/sec, the AB08 ground motions are presented for the NEHRP C site condition. Both Zea06 and Zea16 are also defined based on a binned site classification. For the V_{S30} value of 760 m/sec, their SC I (Rock) site category, which is the combination of NEHRP A and B site conditions (Zhao et al., 2006), is used. For the V_{S30} value of 400 m/sec, their SC II (Hard Soil site category), which is consistent with the NEHRP C site condition (Zhao et al., 2006), is selected for the comparisons. Both the BCH and BCHU models are defined as a continuous function of V_{S30} values.

The AB08 model was developed as a global model with two additional regionalized versions for Cascadia and Japan. Since these previously published models are compared with global versions of the new models, the comparison with AB08 is based on the global version of that model. Although the AM09 model was developed specifically for Cascadia interface events, it is compared to the global version of the three new NGA-Sub models

given that the AM09 model has been used along with other global models for seismic hazard studies in the Cascadia region. The Zea06 and Zea16 are both based on predominately Japanese data. However, because these models have typically been applied globally, comparisons will be presented with the global models.

The BCH global model is presented in the comparisons. For the attenuation curve plots, only the forearc ground motions are compared given the lack of a backarc version for the new NGA-Sub GMMs, even though for the larger distances up to 1000 km, one would expect that the sites would primarily be located in the backarc region. Finally, the BCHU model was developed specifically for application by the USGS for Cascadia earthquakes rather than a global application. Similar to the inclusion of the AM09 model with the global models, the BCHU model is also included in the global-model comparisons given the use of both regional and global models in Cascadia. For both the BCH and BCHU models, the upper and lower versions of these models that account for epistemic uncertainty are also included in the comparison figures and digital files.

As noted earlier, the comparisons presented in this article (i.e. both in the graphical comparison plots and as well in the associated electronic files) do not fully span the wide range of parameters that may be important for specific applications. The focus of this article is to present the comparison of GMMs for global application and as well as Cascadia and Japan. Comparisons for other regions are contained in the associated electronic files. Through the observations and understanding of these new NGA-Sub GMMs and with any additional comparison studies, it is anticipated that the evaluation and application of these new models can be technically informed.

Interface events attenuation curves and spectra

Comparison results for the global versions of the NGA-Sub GMMs are presented for magnitude 7, 8, and 9 interface events for the two defined site conditions with V_{S30} values of 400 m/sec and 760 m/sec. For the attenuation curves, the distance range is shown as 10–1000 km. It should be noted that these large distances fall outside of the recommended application range of some of the GMMs but are shown to present the extrapolation of these models with other models which are defined out to 1,000 km. For the response spectra plots, results are provided for two distances of 75 and 200 km. The depth to the top of the rupture required for the KBCG model was assigned to be 10 km, and the hypocentral and Moho depth for the SMK model were assigned to be 20 and 30 km, respectively.

Attenuation curves for a **M**8 interface event are shown in Figure 1 for PGA and T = 1 sec spectral acceleration, both for a V_{S30} value of 400 m/sec. Similar attenuation curves are plotted in Figure 2 for a V_{S30} value of 760 m/sec. The global curves from the AG, KBCG, and PSBAH models are compared with the suite of selected other GMMs. Overall, there is comparable agreement between the GMMs for distances less than about 200 km and a larger discrepancy between attenuation curves for greater distances. The observed saturation of the AB08 model for distances less than about 50 km is based on the extrapolation of that model for short distances with limited data. Additional comparison plots are provided in the electronic files (Supplemental Appendix A) for the other magnitudes, spectral periods, and individual regions.

The comparisons of **M**8 response spectra for the full spectral period range of 0.01 – 10 s are presented in Figure 3 (distance of 75 km) and Figure 4 (distance of 200 km) for the two V_{S30} values for the global version of the NGA-Sub models. In general, the NGA-Sub
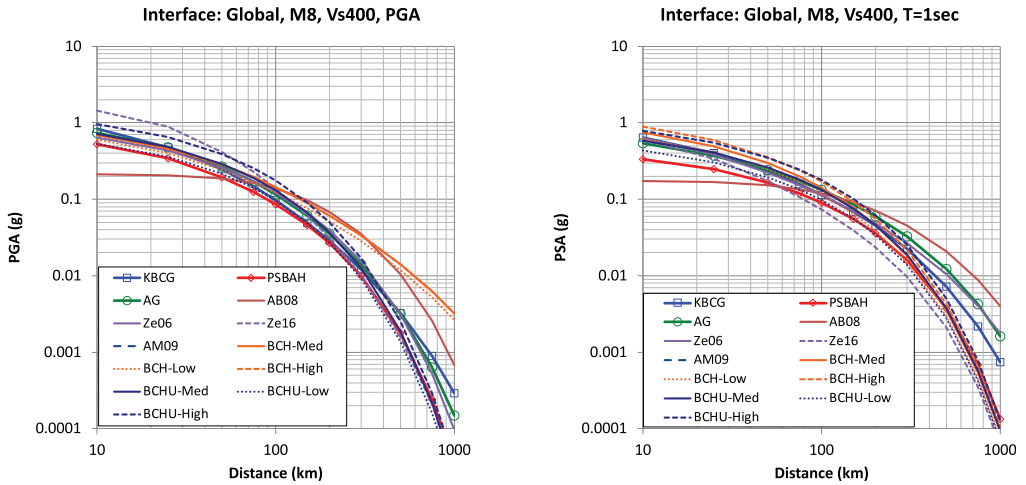
Figure 1. Comparison of attenuation curves for a **M**8 interface event (Ztor = 10 km) for PGA (left panel) and T = 1 sec spectral acceleration (right panel) for V$_{S30}$ = 400 m/sec (see *Interface-Atten-Global-EQSRev001.xlsx*).
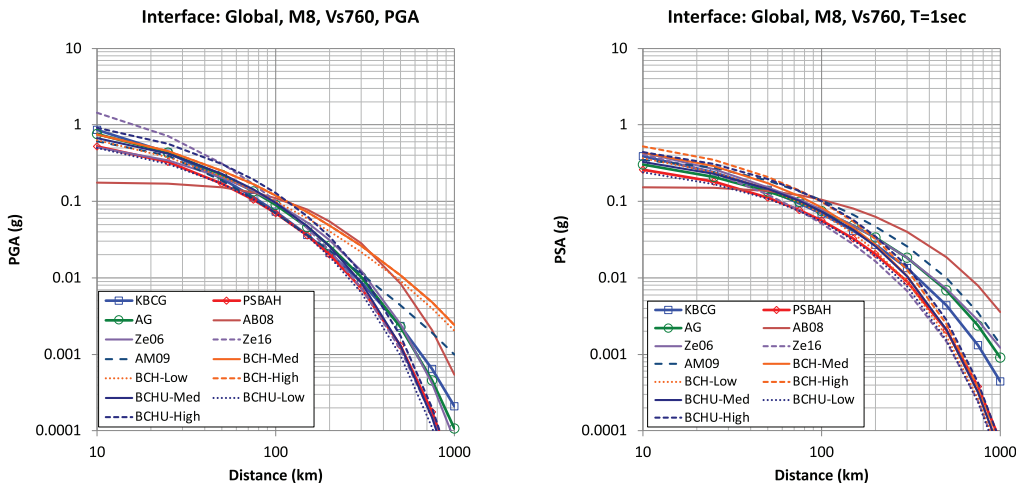

Figure 2. Comparison of attenuation curves for a **M**8 interface event (Ztor = 10 km) for PGA (left panel) and T = 1 sec spectral acceleration (right panel) for V$_{S30}$ = 760 m/sec (see *Interface-Atten-Global-EQSRev001.xlsx*).

models are within about a factor of 2 of each other, whereas the range of all of the compared GMMs falls in the range of 3 – 4, with a large discrepancy observed for the greater distance of 200 km and V$_{S30}$ of 760 m/sec.

Given that the SMK model is a regional model for Japan, a comparison of the spectra from an **M**8 interface event at a distance of 75 km is shown in Figure 5 for the V$_{S30}$ values of 400 and 760 m/sec. For these comparisons, the NGA-Sub GMMs are plotted both with their respective global versions (solid lines with symbols) and the regionalized versions
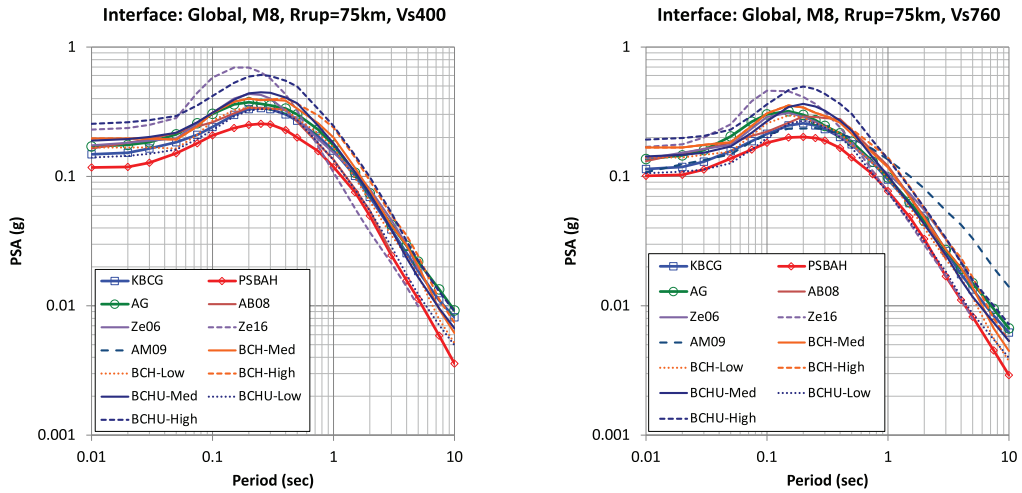
Figure 3. Comparison of response spectra for a **M**8 interface event (Ztor = 10 km) at a distance of 75 km for V_{S30} = 400 m/sec (left panel) and for V_{S30} = 760 m/sec (right panel) (see *Interface-Spectra-Global-EQSRev001.xlsx*).
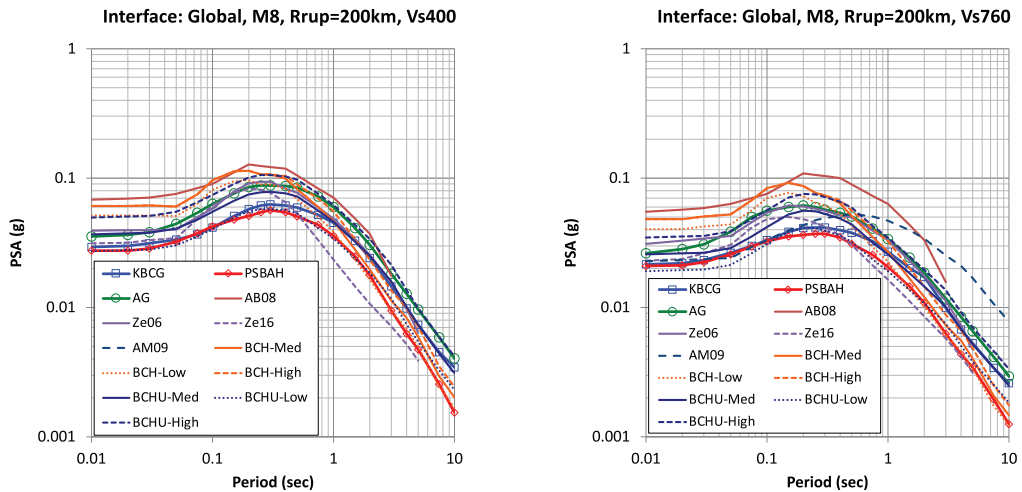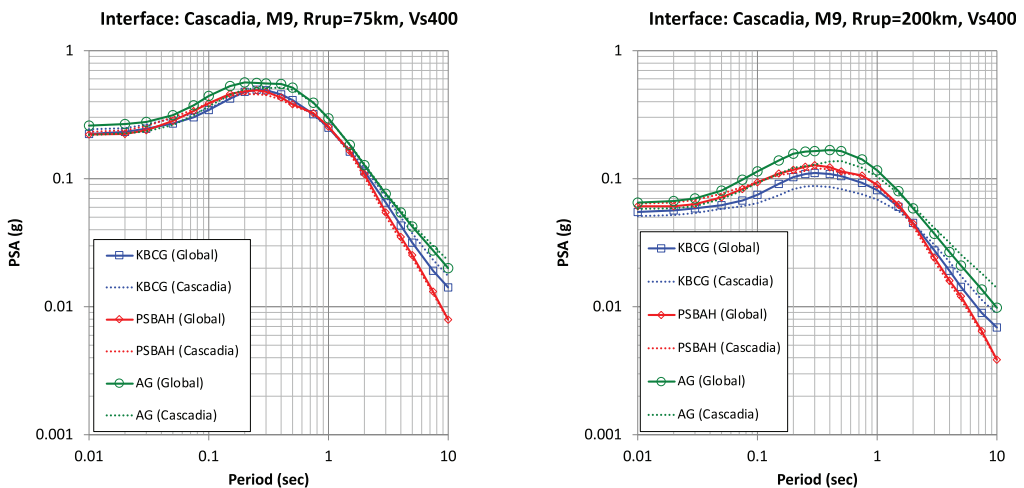

Figure 4. Comparison of response spectra for a **M**8 interface event (Ztor = 10 km) at a distance of 200 km for V_{S30} = 400 m/sec (left panel) and for V_{S30} = 760 m/sec (right panel) (see *Interface-Spectra-Global-EQSRev001.xlsx*).

specific to Japan (dashed lines). For the KBCG and PSBAH models, the different magnitude scaling breakpoint values for the two main tectonic plates in Japan (i.e. Pacific plate and the Philippine Sea plate) are plotted separately. Overall, the agreement between the SMK model and the regionalized NGA-Sub GMMs is good, with a similar factor of approximately 2. For the short-period range, the Japan regionalized models predict higher ground motions than the global versions of the GMMs. For longer spectral periods, these
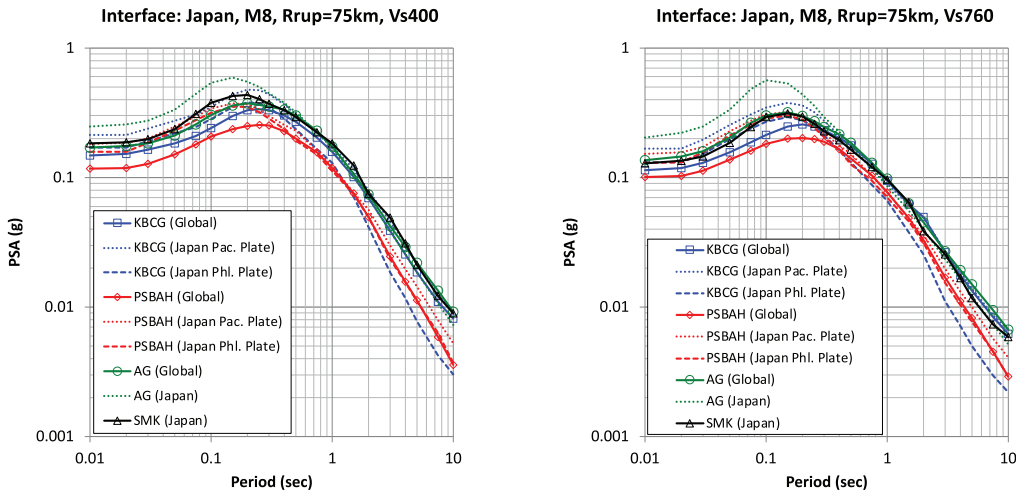
Figure 5. Comparison of response spectra for a **M**8 interface event (Ztor = 10 km) for the global versions (solid lines with symbols) and Japan regional versions (dashed lines) at a distance of 75 km for V_{S30} = 400 m/sec (left panel) and for V_{S30} = 760 m/sec (right panel) (see *Interface-Spectra-Japan-EQSRev001.xlsx*).

Figure 6. Comparison of response spectra for a **M**9 interface event (Ztor = 10 km) for the global versions (solid lines with symbols) and Cascadia regional versions (dashed lines) at a distance of 75 km (left panel) and 200 km (right panel) for V_{S30} = 400 m/sec (see *Interface-Spectra-Cascadia-EQSRev001.xlsx*).

comparisons indicate equal ground motions or slightly lower ground motions from the regional models compared to the global models.

The comparison for the Cascadia **M**9 interface event with a V_{S30} value of 400 m/sec is plotted in Figure 6 for the two distances of 75 km (left panel) and 200 km (right panel). The Cascadia region is limited in the number of interface events selected for the development of the GMMs, but each model recommends an adjustment relative to their global

versions. The regional adjustment for the PSBAH model is small compared to the other two NGA-Sub models (AG and KBCG), but the overall agreement between the three regional Cascadia models is favorable and more comparable than that of the global models.

Interface events magnitude scaling

All of the four NGA-Sub GMMs contain a magnitude scaling breakpoint (i.e. see Table 3) to account for a change in the magnitude scaling and saturation observed in empirical data and simulations. This feature was also modeled in previous GMMs such as the BC Hydro (Abrahamson et al., 2016) model as well as for crustal GMMs (e.g. see Gregor et al., 2014). For the comparisons, the magnitude-scaling from the global NGA-Sub models and the selected comparison GMMs for interface events at a distance of 75 km with a V_{S30} value of 760 m/sec are plotted in Figure 7. The SMK model is also included in these comparison figures. The magnitude-scaling observed in Figure 7 is fairly similar for the NGA-Sub models, with the largest difference being for the SMK model at the longer spectral period of 3 s. For this case, the change in the magnitude scaling slope is flatter than for the other models, leading to higher ground motions for these larger magnitude cases (i.e. greater than about 8.5). Note that for the AM09 and AB08 models, the curves are only plotted for magnitudes equal to or greater than 7, given their unfavorable behavior for smaller magnitudes, which are extrapolations of these models beyond the recommended range and/or range of the data used in their development.

Interface events depth scaling

Only the KBCG model contains a function for the depth to the top of the rupture (Z_{TOR}) from interface events. This dependence has a stronger influence on short-period ground motions than on longer period ground motions. To illustrate this, the comparison of ground motions as a function of Z_{TOR} is plotted in Figure 8 for the suite of GMMs. Results for T = 0.01 sec (left panel) and 1.0 sec (right panel) are presented for a **M**8 event at a distance of 75 km and with V_{S30} = 760 m/sec. For all of the models except the KBCG model, the ground motion values are not dependent on Z_{TOR}.

Slab events attenuation curves and spectra

For the slab event comparisons, ground motions are computed for magnitudes 6, 7, and 8 for the same two V_{S30} values of 400 and 760 m/sec. Attenuation curves are provided over the distance range of 50 – 1000 km and the spectra comparisons are for two representative distances of 75 and 200 km. The depth to the top of the rupture for the KBCG and AG models was assigned as 50 km, and the hypocentral depth for the PSBAH and SMK models is magnitude dependent with values of 50, 60, and 70 km for magnitudes of 6, 7, and 8.

Attenuation curves for a **M**7 slab event are shown in Figure 9 for PGA and T = 1 sec spectral acceleration, both for a V_{S30} value of 400 m/sec. Similar attenuation curves are plotted in Figure 10 for a V_{S30} value of 760 m/sec. Overall, there is general agreement between the NGA-Sub GMMs for distances less than about 400 km for PGA and at even larger distances for the 1 sec case. In comparison with the other GMMs, the BCHU (Abrahamson et al., 2018) model is lower than the other models, but it should be noted that the BCHU model is a Cascadia specific model and, as noted in the development of the Cascadia regionalized models, lower ground motions are estimated relative to the
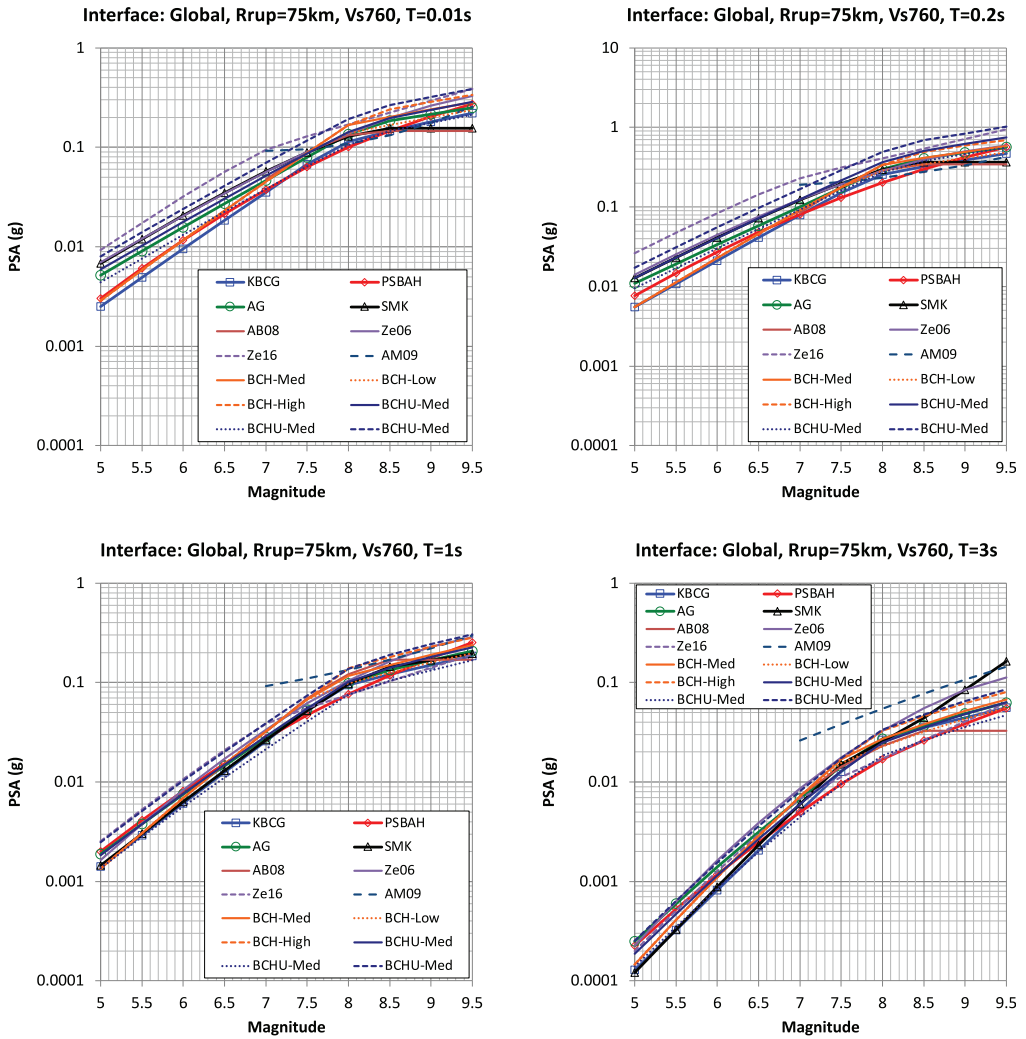
Figure 7. Comparison of magnitude dependence of ground motions at a distance of 75 km and V_{S30} = 760 m/sec (Ztor = 10 km) for T = 0.01 sec (upper left), T = 0.2 sec (upper right), T = 1.0 sec (lower left) and T = 3.0 sec (lower right).

global versions of the models, especially for short spectral periods. The full set of comparisons and digital values are contained in the associated electronic files (Supplemental Appendix A) for other magnitudes, spectral periods, and individual regions.

The comparisons of **M**7 global response spectra for the full spectral period range of 0.01 – 10 s are presented in Figure 11 (distance of 75 km) and Figure 12 (distance of 200 km) for the two V_{S30} values for the NGA-Sub models. These comparisons show a similarity in the estimated ground motions (variations of 50% or less) from just the three NGA-Sub GMMs. When the other GMMs are included as shown in Figures 11 and 12, the variability of estimated ground motions is larger in the short period range, especially when including
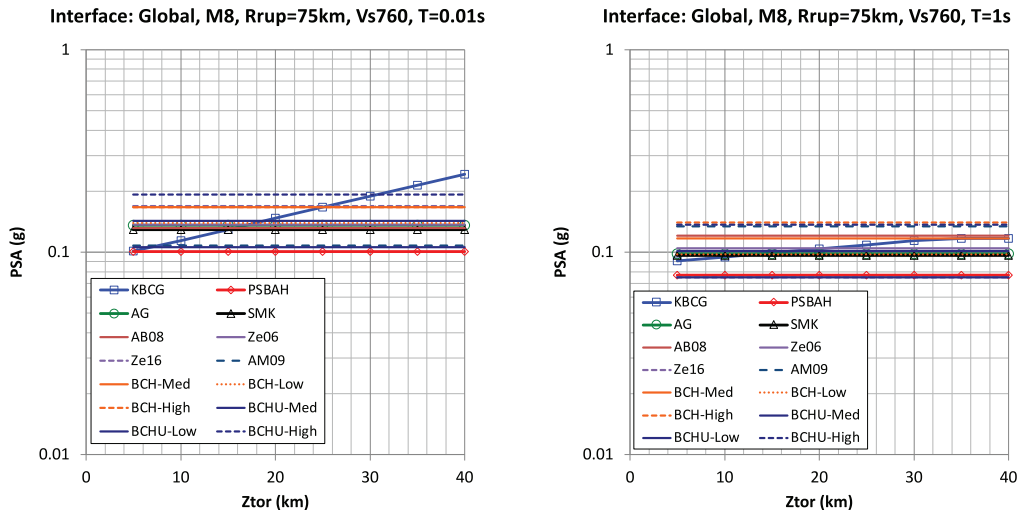
Figure 8. Comparison of Z_{TOR} dependence of ground motions for a M8 interface event at a distance of 75 km and V_{S30} = 760 m/sec for T = 0.01 sec (left panel) and T = 1.0 sec (right panel).
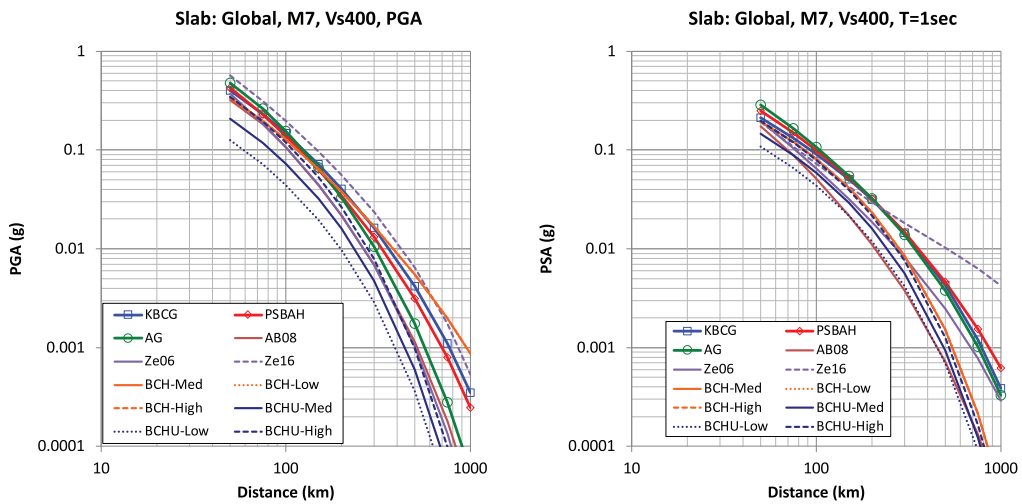
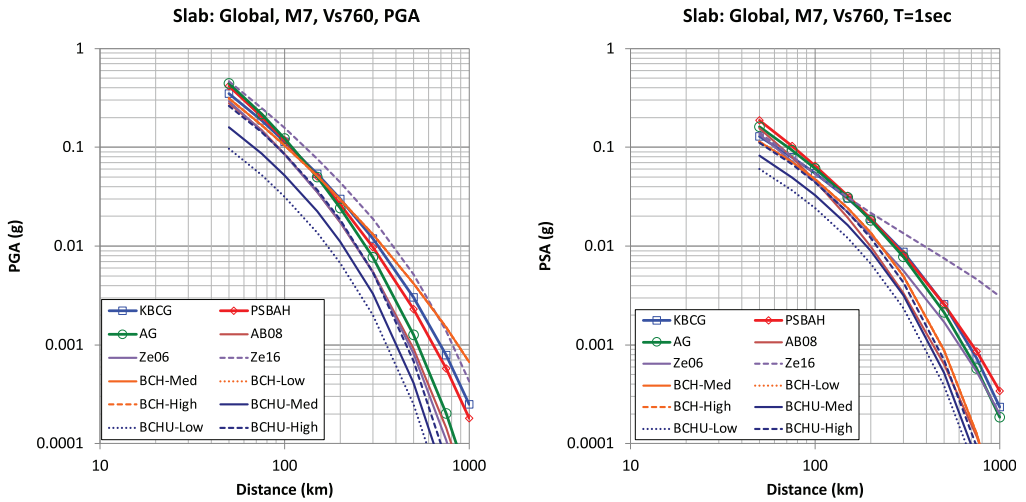**Figure 9.** Comparison of attenuation curves for a **M**7 slab event (Ztor = 50 km) for PGA (left panel) and T = 1 sec spectral acceleration (right panel) for V_{S30} = 400 m/sec (see *Slab-Atten-Global-EQSRev001.xlsx*).

the BCHU model, which is a regionalized Cascadia GMM. For the longer spectral periods, the suite of GMMs predicts comparable ground motions.

For the Japan region, the spectra comparisons, including the SMK model, are plotted in Figure 13 for an **M**7 slab event at a distance of 75 km for just the NGA-Sub models. Both the V_{S30} = 400 m/sec (left panel) and 760 m/sec (right panel) are plotted. Additional comparisons are available in the electronic files. Slightly larger differences (i.e. factors of about 2) are observed between the Japan regionalized NGA-Sub models and the NGA-

Figure 10. Comparison of attenuation curves for a **M**7 slab event (Ztor = 50 km) for PGA (left panel) and T = 1 sec spectral acceleration (right panel) for V_{S30} = 760 m/sec (see *Slab-Atten-Global-EQSRev001.xlsx*).
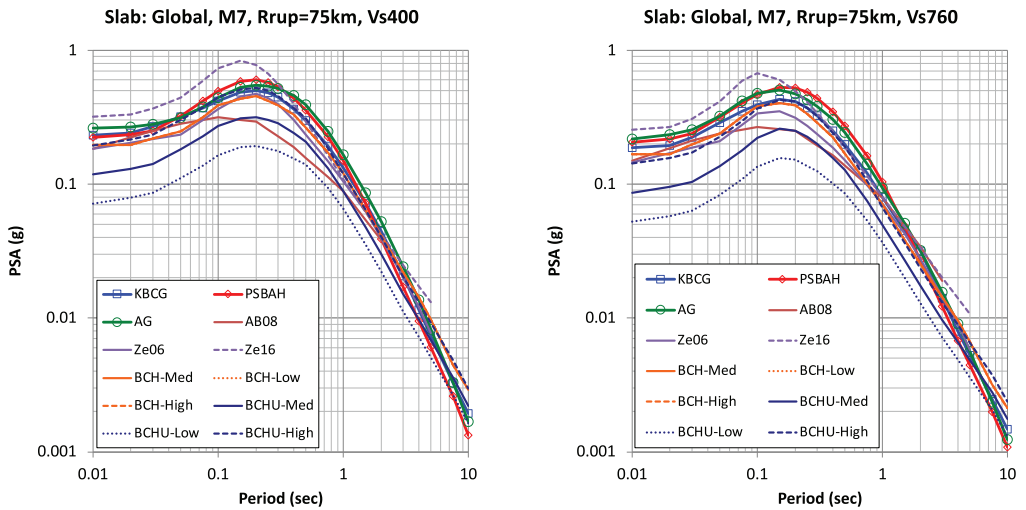
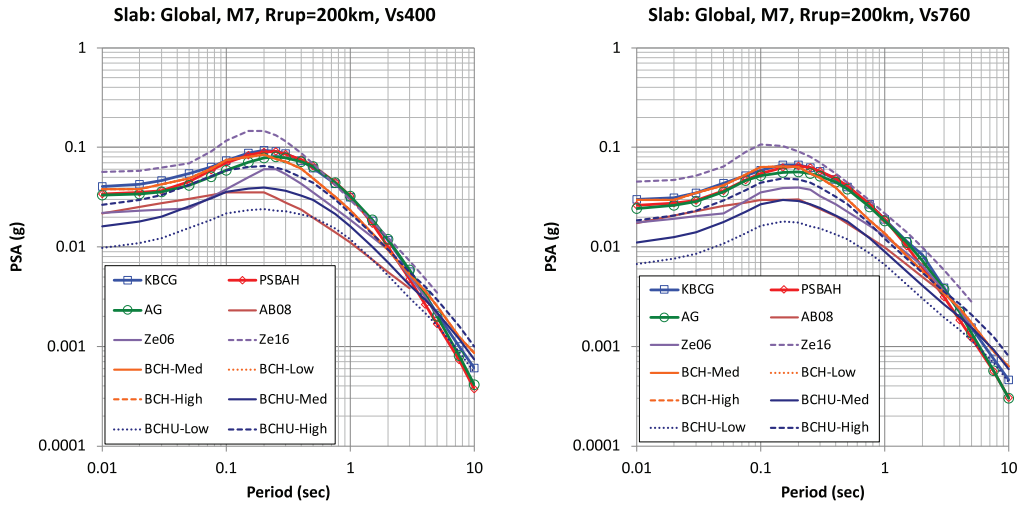**Figure 11.** Comparison of response spectra for a **M**7 slab event (Ztor = 50 km) at a distance of 75 km for V_{S30} = 400 m/sec (left panel) and for V_{S30} = 760 m/sec (right panel) (see *Slab-Spectra-Global-EQSRev001.xlsx*).

Sub global models. Note that in these comparison plots, the selected magnitude of 7 is below the magnitude scaling breakpoint for the KBCG and PSBAH models, and the spectra from the Pacific and Philippine Sea plate cases are identical. The impact of the different magnitude-scaling breakpoint magnitudes (i.e. see Table 3) for these two models can be observed in the additional comparisons (i.e. **M**8 case) contained in the electronic files (Supplemental Appendix A).

Slab: Global, M7, Rrup=200km, Vs400

Slab: Global, M7, Rrup=200km, Vs760

Figure 12. Comparison of response spectra for a **M**7 slab event (Ztor = 50 km) at a distance of 200 km for V_{S30} = 400 m/sec (left panel) and for V_{S30} = 760 m/sec (right panel) (see *Slab-Spectra-Global-EQSRev001.xlsx*).

Slab: Japan, M7, Rrup=75km, Vs400

Slab: Japan, M7, Rrup=75km, Vs760
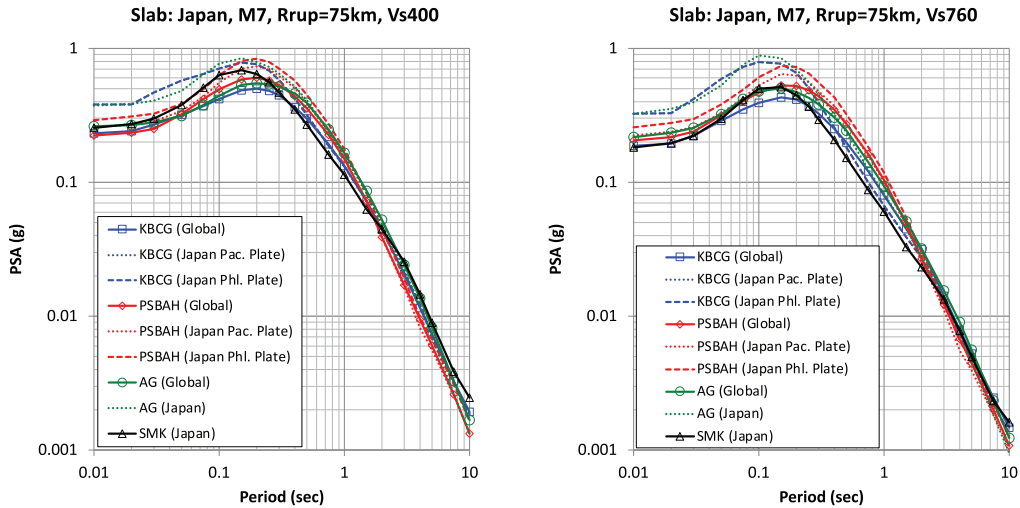
Figure 13. Comparison of response spectra for a **M**7 slab event (Ztor = 50 km) for the global versions (solid lines with symbols) and Japan regional versions (dashed lines) at a distance of 75 km for V_{S30} = 400 m/sec (left panel) and for V_{S30} = 760 m/sec (right panel) (see *Slab-Spectra-Japan-EQSRev001.xlsx*).

The comparison for the Cascadia **M**7 slab event with a V_{S30} value of 760 m/sec is plotted in Figure 14 for the two distances of 75 km (left panel) and 200 km (right panel). For spectral periods greater than about 2 sec, there is close agreement between the three NGA-Sub models, both for the global and Cascadia regionalized cases. However, for shorter spectral periods, the Cascadia models are slightly more dispersed (i.e. differences
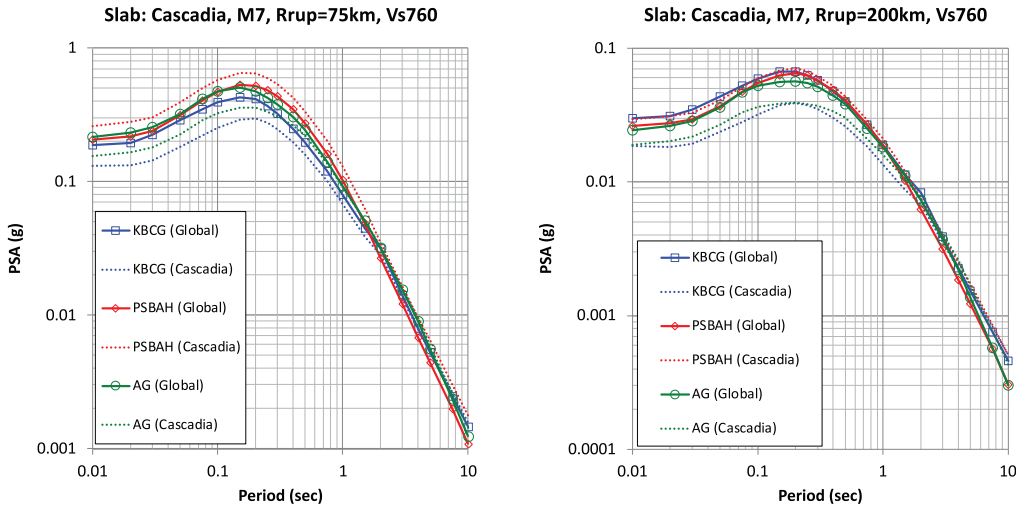
Figure 14. Comparison of response spectra for a **M**7 slab event (Ztor = 50 km) for the global versions (solid lines with symbols) and Cascadia regional versions (dashed lines) at a distance of 75 km (left panel) and 200 km (right panel) for V_{S30} = 400 m/sec (see *Slab-Spectra-Cascadia-EQSRev001.xlsx*).

of about 50%), with the KBCG and AG models estimating lower ground motions than the PSBAH model. The relative increase in the PSBAH model compared to the other two models is more pronounced for larger magnitudes (e.g. see the **M**8 comparisons in the Supplemental Appendix A) and for the V_{S30} value of 760 m/sec compared to the results for V_{S30} of 400 m/sec.

Slab events magnitude scaling

Similar to the magnitude scaling for interface events, all of the NGA-Sub models include a breakpoint in the magnitude scaling slope for slab events (i.e. see Table 3). For the slab comparisons, the ground motions for slab events at a distance of 75 km with a V_{S30} value of 760 m/sec are plotted in Figure 15 as a function of magnitude. Overall, the agreement between the global NGA-Sub GMMs and the other GMMs is comparable, with the exception of the BCHU (Abrahamson et al., 2018) model, which should be noted was developed specifically for Cascadia and has a lower magnitude scaling dependence on magnitude. Also note that for magnitudes greater than 8.0, the AB08 model is fully saturated (i.e. no increase in ground motion values for magnitudes larger than 8).

Slab events depth scaling

A strong source-depth dependence has been noted in previous GMMs for slab events (e.g. Abrahamson et al., 2016). This dependence is greater for short spectral periods than for longer periods. Comparisons of estimated ground motions for T = 0.01 sec (upper left), T = 0.2 sec (upper right), 1.0 sec (lower left) and 3.0 sec (lower right) are presented in Figure 16. These ground-motion curves are plotted as a function of Z_{TOR} for **M**7 slab earthquakes at a distance of 75 km and with a V_{S30} value of 760 m/sec. For these comparisons, the Z_{TOR} for the AG and KBCG models and the hypocentral depth (Z_{HYP}) for the PSBAH and SMK models were assumed to be equal. For Z_{TOR} values of greater than
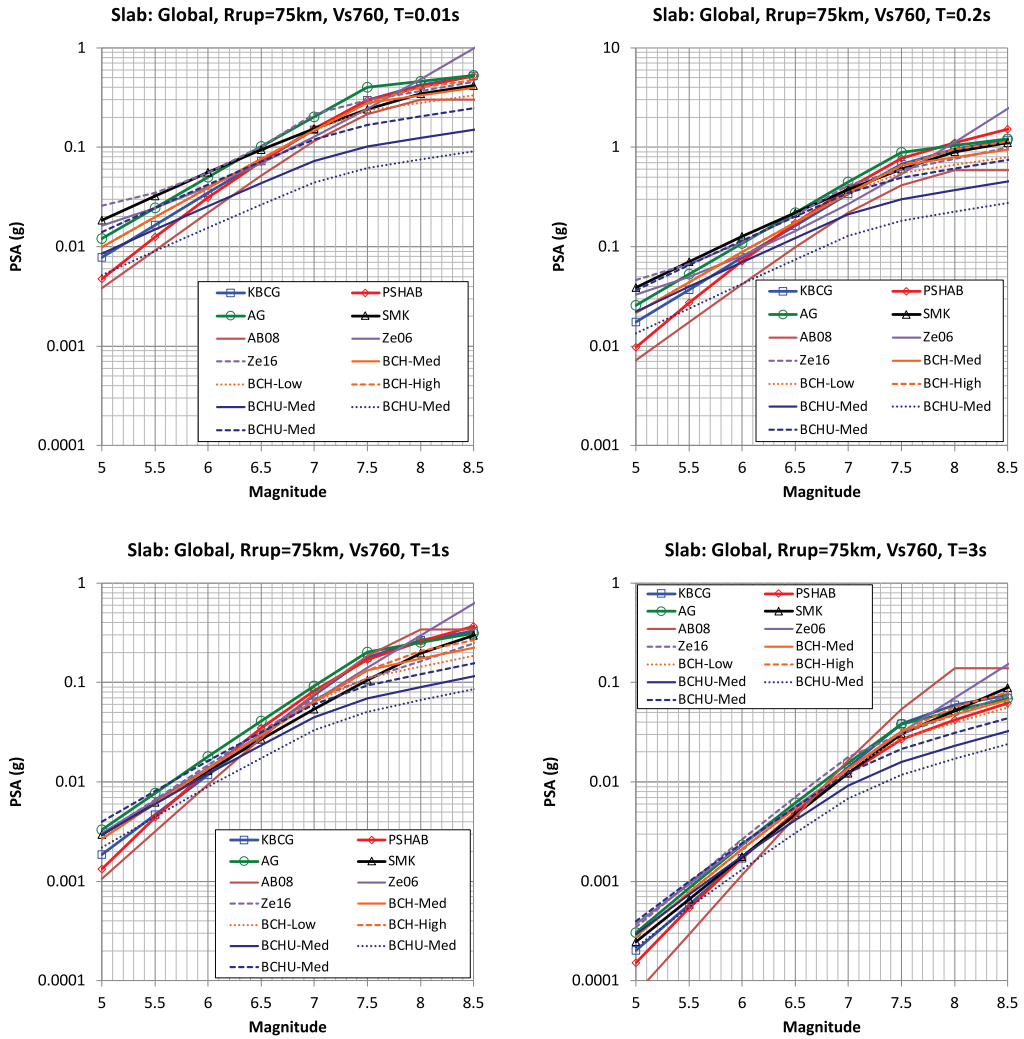
Figure 15. Comparison of magnitude dependence of ground motions at a distance of 75 km and V_{S30} = 760 m/sec (Ztor = 50 km) for T = 0.01 sec (upper left), T = 0.2 sec (upper right), T = 1.0 sec (lower left) and T = 3.0 sec (lower right).

about 70 km, the KBCG and PSBAH models saturate (i.e. relatively no increase in ground motions with increasing Z_{TOR} or Z_{HYP}), AG slightly increases, and the SMK model increases at the same rate as for smaller distances.

Basin amplification

All four of the NGA-Sub GMMs contain a basin amplification term to account for the ground motion response associated with the deeper structure not accounted for with the site response function dependent on the V_{S30} parameter. These factors are applicable to both interface and slab events, and for the AG, KBCG, and PSBAH models, the amplification is relative to a differential depth defined as depth minus a default $Z_{2.5}$ or $Z_{1.0}$ depth
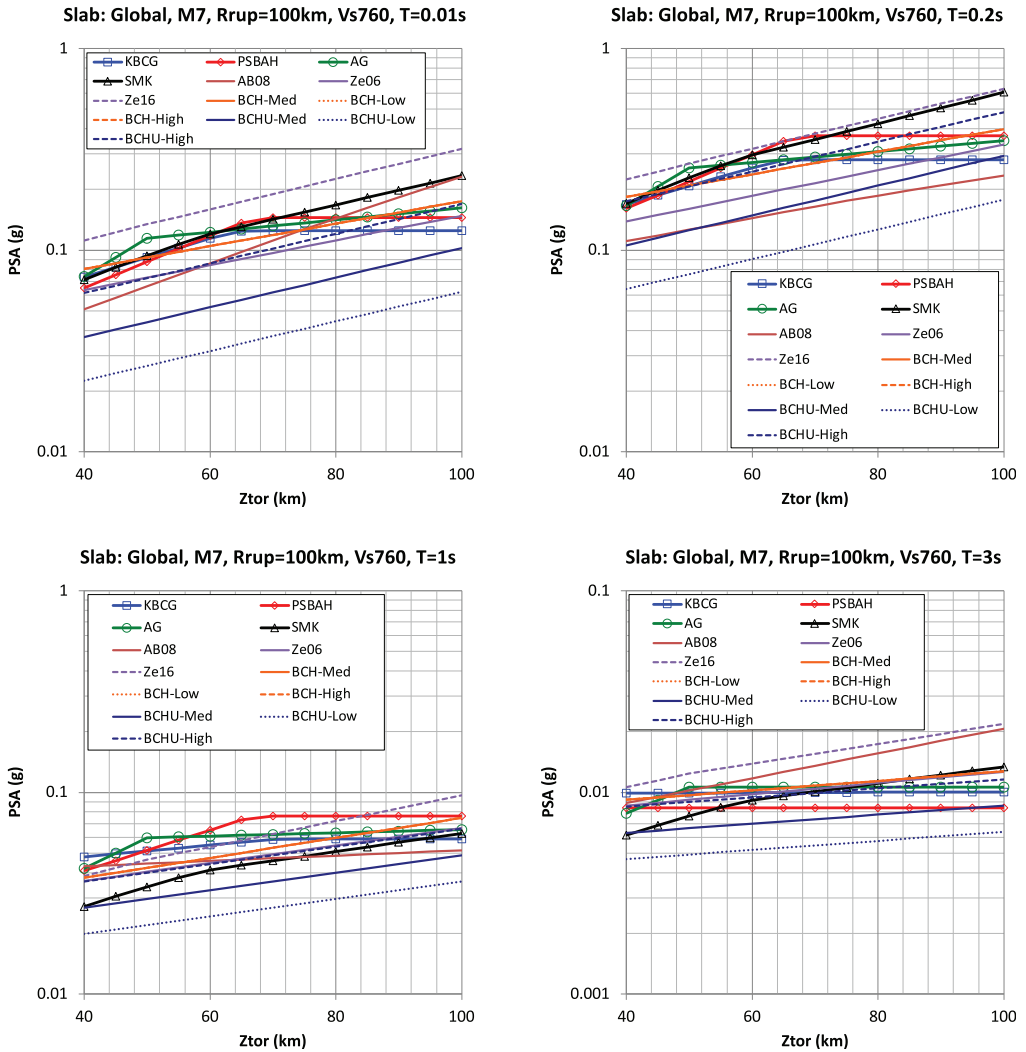
Figure 16. Comparison of Z_{TOR} dependence of ground motions for a **M**7 slab event at a distance of 75 km and V_{S30} = 760 m/sec for T = 0.01 sec (upper left), T = 0.2 sec (upper right), T = 1.0 sec (lower left), and T = 3.0 sec (lower right).

value. The SMK model is based directly on the $Z_{2.5}$ parameter value. Separate empirical relationships for the other NGA-Sub GMMs were developed as part of the basin amplification models. For Japan and Cascadia, the NGA-Sub GMMs are parameterized based on the $Z_{2.5}$ parameter. For the KBCG model, two additional basin amplification regions are developed for Taiwan and New Zealand, and these models are defined based on the $Z_{1.0}$ parameter. Given the regional variation within Cascadia for sites located within the Seattle basin and other basins, the KBCG model differentiates the Cascadia basin amplification into separate specific basins.

The basin amplification factors for an interface **M**8 event at a distance of 75 km with a V_{S30} = 400 m/sec for Japan are plotted in Figure 17. These spectral ratios are relative to
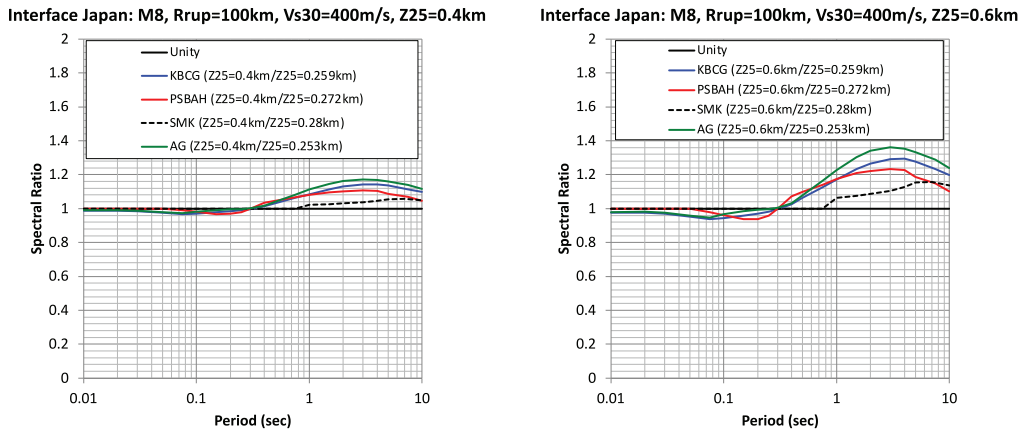
Interface Japan: M8, Rrup=100km, Vs30=400m/s, Z25=0.4km

Interface Japan: M8, Rrup=100km, Vs30=400m/s, Z25=0.6km

Figure 17. Comparison of basin amplification dependence of ground motions for a Japan **M**8 interface event (Z_{tor} = 10 km) at a distance of 75 km and V_{S30} = 400 m/sec for $Z_{2.5}$ = 0.4 km (left panel) and $Z_{2.5}$ = 0.6 km (right panel).
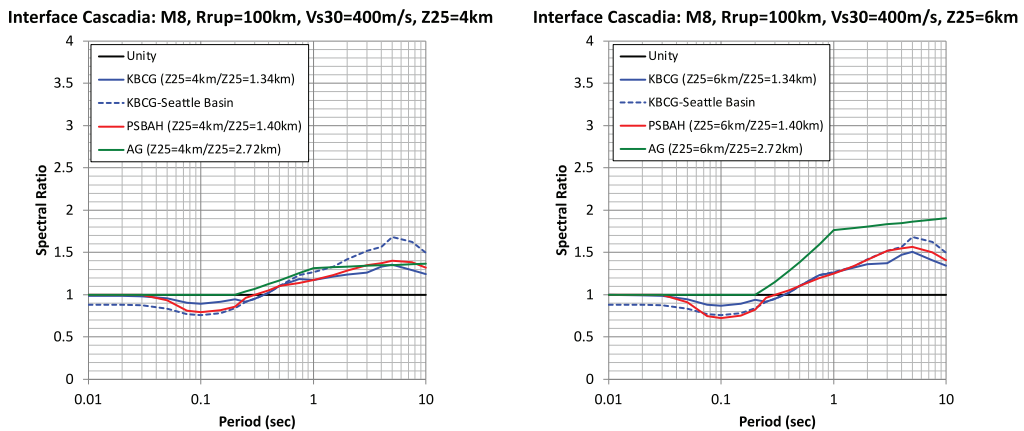
Interface Cascadia: M8, Rrup=100km, Vs30=400m/s, Z25=4km

Interface Cascadia: M8, Rrup=100km, Vs30=400m/s, Z25=6km

Figure 18. Comparison of basin amplification dependence of ground motions for a Cascadia **M**8 interface event (Z_{tor} = 10 km) at a distance of 75 km and V_{S30} = 400 m/sec for $Z_{2.5}$ = 0.4 km (left panel) and $Z_{2.5}$ = 0.6 km (right panel).

the default $Z_{2.5}$ parameter value (i.e. as indicated in the denominator value listed in the legend for each curve) for each of the four GMMs based on the V_{S30} value of 400 m/sec. The SMK model predicts lower basin amplification than the other three NGA-Sub models and only impacts the longer spectral periods greater than 1.0 s. It is also observed that the AG, KBCG, and PSBAH models also predict a slight de-amplification for spectral periods less than about 0.3 s.

For Cascadia, a comparison of basin amplification factors (i.e. spectral ratio of ground motions for basin site divided by non-basin site) is plotted in Figure 18 for a scenario interface event (**M**8 at 75 km distance and V_{S30} = 400 m/sec). The KBCG model is separated into Seattle basin sites and non-Seattle basin sites. The PSBAH and AG models are defined for a general basin in the PNW, which includes the Seattle basin. For the KBCG
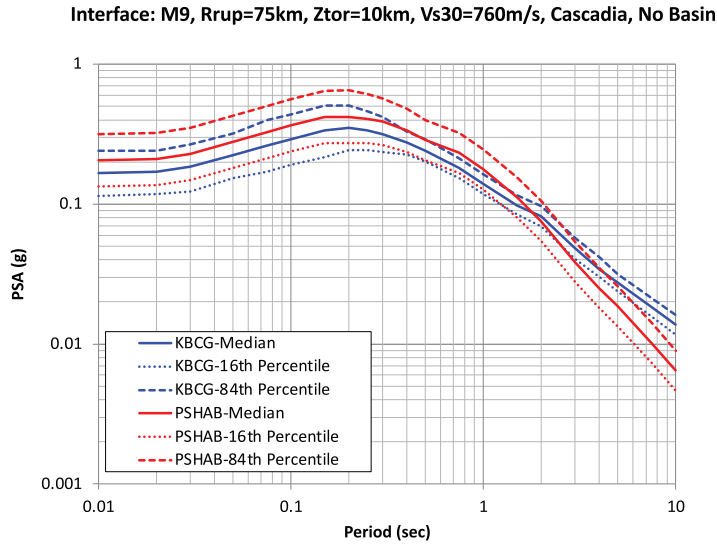
Interface: M9, Rrup=75km, Ztor=10km, Vs30=760m/s, Cascadia, No Basin

Figure 19. Comparison of epistemic uncertainty for a Cascadia **M**9 interface event (Ztor = 10 km) at a distance of 75 km and V_{S30} = 760 m/sec (no basin) for the KBCG and PSBAH models.

model, the Seattle basin model has larger amplification than the other KBCG general basin models in the longer spectral period range. In the shorter period range, both the Seattle basin model and the general basin model predict de-amplification. These results for basins located in the Cascadia region show larger differences than the results for Japan.

Epistemic uncertainty

The GMMs of Abrahamson et al. (2016, 2018) included an epistemic variation of the base model. The PSBAH model provides a region-dependent epistemic model (Parker et al., 2020, 2021). For the KBCG model, the epistemic uncertainty can be estimated from a sample of 800 posterior distributions of the model coefficients developed based on the availability of 800 correlated regression coefficients developed as part of Bayesian regression analysis (Kuehn et al., 2020, 2021). This sampling can be performed for either the global model or specific regionalized models. AG (Abrahamson and Gülerce, 2020, 2021) recommends utilizing additional epistemic uncertainty with the global model based on the range of the region-specific scaling relations and estimated ground motions.

As an example, the recommended epistemic uncertainty for the 16th and 84th percentiles for the KBCG and PSBAH models is plotted in Figure 19 for a Cascadia scenario event. This event is an interface **M**9 earthquake at a distance of 75 km with a V_{S30} value of 760 m/sec. Both models predict similar epistemic factors of about 50% of the mean estimated spectrum. In addition to this regional epistemic uncertainty associated with the KBCG and PSBAH models, it is expected that an evaluation of the model-to-model uncertainty will be performed in the future. This will allow for the potential development of an applicable epistemic model that could be implemented for seismic hazard studies that is similar to how the Al Atik and Youngs (2014) model is typically implemented for the NGA-West2 GMMs (Bozorgnia et al., 2014).
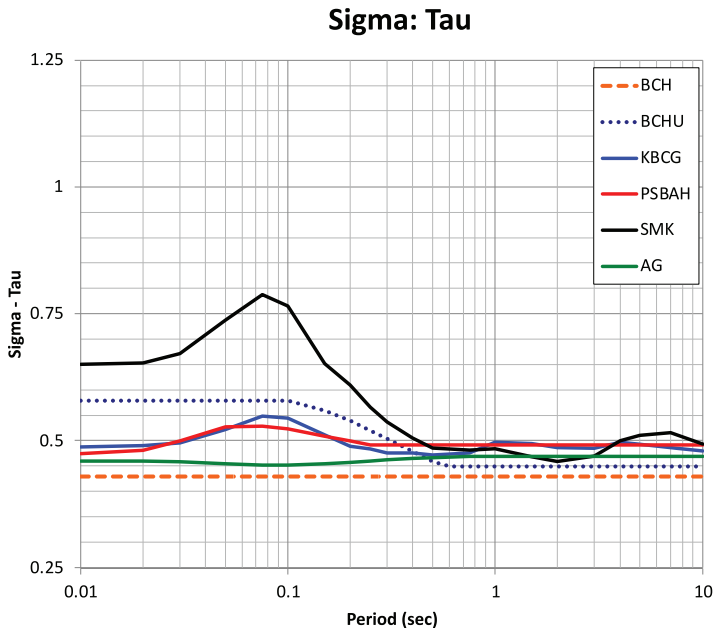
Sigma: Tau

Figure 20. Comparison of between-event standard deviations.

Aleatory variability

The aleatory variability is based on the between-event (τ) and within-event standard deviations (φ) following the structure of Al Atik et al. (2010). Similar to the development of the median GMM, each modeling team investigated, evaluated, and developed an aleatory uncertainty model based on the between-event and within-event variations. For all four models, the between-event variability is independent of predictor variables such as distance, magnitude, and site conditions. For the KBCG and SMK models, the within-event variability is also parameter-independent. For the PSBAH model, the within-event model is defined as a function of distance and V_{S30}. Note that a single-station standard deviation is also being developed for the PSBAH model but is not currently available for the other NGA-Sub models. For the AG model, the within-event variability is dependent on the distance and the specific region.

Comparisons of the between-event standard deviations from the BCH and BCHU models and the four NGA-Sub models are plotted in Figure 20. The within-event standard deviations are compared in Figure 21 for two distances of 100 and 400 km, both for a V_{S30} value of 400 m/sec. Both a strong distance dependence and a regionalization of the AG within-event standard deviations are observed in Figure 21. Combining the between-event and within-event standard deviations produces the total aleatory standard deviations shown in Figure 22 for the two distances. In general, the AG model is comparable to the previous BCH model, which is smaller than the BCHU model for the shorter distance of 100 km and slightly larger at the 400 km distance. For the other three models for the 100 km distance case, the total standard deviations are more similar to the BCHU values than the BCH values and fall both above and below the BCHU values as a function of spectral period. For the larger 400 km distance case, the total standard deviations from
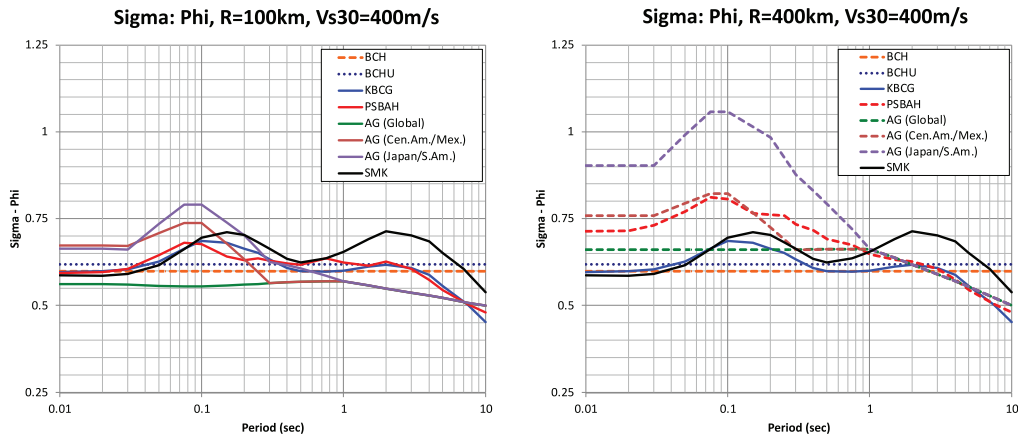
Figure 21. Comparison of within-event standard deviations for V_{S30} = 400 m/sec and distances of 100 km (left panel) 400 km (right panel).
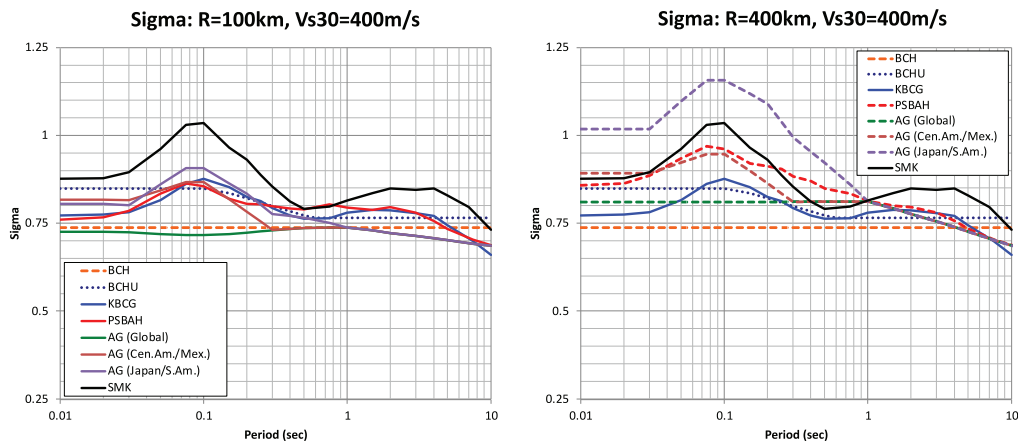

Figure 22. Comparison of total standard deviations for V_{S30} = 400 m/sec and distances of 100 km (left panel) 400 km (right panel).

these three models are larger than the BCHU model except at the longer spectral periods where the AG, KBCG, and PSBAH all fall below the BCHU and BCH models.

Example Cascadia PSHA calculation

To illustrate the potential impacts of incorporating these new NGA-Sub GMMs, PSHA were performed for two sites in Washington State in the Pacific Northwest region, where hazard is impacted by the Cascadia subduction zone (i.e. both interface and slab sources). The first site is for a location in downtown Seattle; the second site is located in the town of Centralia, Washington. The locations of these two sites are plotted in Figure 23. The PSHA results presented in this section for these two sites are only meant to illustrate the potential impact from the use of these new models. It is expected that as part of the
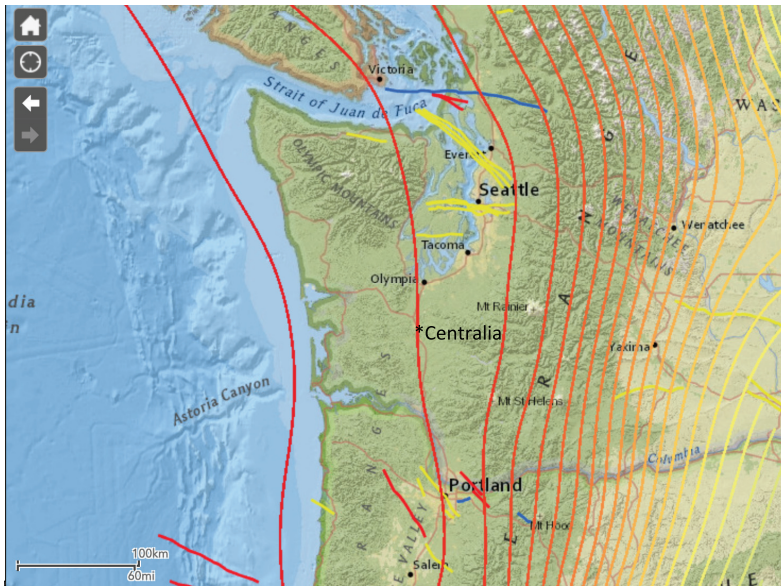
Figure 23. Map showing the location of the two example sites (Seattle and Centralia) used in the PSHA along with the crustal faults (red and yellow lines) and subducting Cascadia subduction zone plate depth contours starting at 20 km depth off the coast and increasing depths of 20 km moving east.
Base map and faults from USGS Quaternary Fault GIS webviewer: http://usgs.maps.arcgis.com/apps/webappviewer/index.html

implementation of these new NGA-Sub GMMs for either sites in the Pacific Northwest or other global sites, sensitivity studies will be conducted to provide technical support for the use of these new models and any associated logic-tree weights.

Results are computed following the PSHA methodology presented in McGuire (2004) using the seismic-source model from the 2014 USGS National Seismic Hazard Model (2014 NSHM; Petersen et al., 2014). As part of the seismic source model for the recently released 2018 NSHM (Petersen et al., 2020), Cascadia interface seismic source modeling is the same as the 2014 model. The deeper slab events have been updated based on a more recent seismicity catalog (Petersen et al., 2020), but these changes would not be expected to change the observations from these example PSHA calculations, which are focused on the differences in the GMMs rather than any seismic source characterization changes. This USGS source model consists of crustal faults (e.g. the Seattle fault and other regional faults), and both large interface events and deeper slab events associated with the Cascadia subduction zone. For the Seattle site, the contribution to the total seismic hazard is based on a combination of the local Seattle crustal fault and the interface and slab events. The Centralia site is located closer to the coast and away from any local crustal faults; therefore, the influence from the crustal faults is diminished, and the relative contribution from the interface events is larger than from the deeper slab events.

To isolate the potential impact on the ground motions from using the three Cascadia regionalized NGA-Sub GMMs (i.e. AG, KBCG, and PSBAH), separate PSHA calculations are performed for each individual GMM. Note that additional epistemic uncertainty is not applied to the NGA-Sub GMMs. For the base case to which the results are
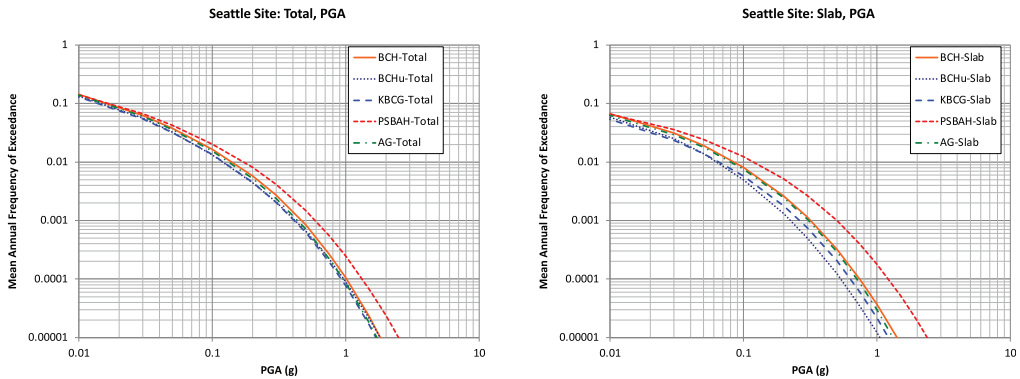
Figure 24. Comparison of total hazard curves separated by subduction GMM (left panel) and slab source hazard curve (right panel) for the Seattle site location for PGA.

compared, the hazard is calculated using the suite of GMMs and associated weights used in the 2014 NSHM. For all crustal seismic sources, the suite of five NGA-West2 models is used with the weighting scheme used in the 2014 NSHM. For the subduction sources (i.e. both interface and slab), the BC Hydro (Abrahamson et al., 2016) model is used given that this model has been widely used for previous seismic hazard studies in the Cascadia region. For the slab event, both the BC Hydro Global and Cascadia region specific models are applied with the recommended weights of 0.7 and 0.3 (Abrahamson et al., 2016), respectively. No additional epistemic model (e.g. Al Atik and Youngs, 2014) is applied to the crustal GMMs or to the BC Hydro or NGA-Sub models in the PSHA calculations. Since the SMK model was developed solely for application in Japan, it is not considered in these example calculations.

All calculations were performed for a V_{S30} value of 760 m/sec and for a site that is not located in a basin. Note that the Seattle site is clearly located in the Seattle basin; however, given that the BCH model does not include an adjustment for basin locations, the PSHA calculations are based on the site not being located within the Seattle basin. The crustal GMM default values for $Z_{1.0}$ and $Z_{2.5}$ given the V_{S30} value of 760 m/sec are applied to the NGA-West2 models. Note that if the example calculations are to be computed for sites located within a basin, the default $Z_{2.5}$ values given a V_{S30} value of 760 m/sec would be different for NGA-Sub GMMs than the crustal GMMs and would need to be accounted for within a PSHA calculation. Results are computed for PGA and spectral periods of 0.2, 1, 3, and 5 s.

The total hazard curves for the Seattle site based on the different subduction GMMs are plotted in the left panel of Figure 24 for PGA. On the right panel is the comparison of only the slab source hazard curves. Similar results are presented in Figure 25 for 1 sec spectral acceleration (i.e. total hazard curves in the left panel and interface source hazard curve in the right panel). These results indicate the implementation of the PSBAH model leads to higher ground motions supported by the observed differences in the slab event predictions, especially for the shorter spectral periods (e.g. as shown in Figure 14 and contained in additional comparisons in the electronic files described in Supplemental Appendix A). The results from the other two NGA-Sub models fall within the range of the results from the BCH and BCHU models.
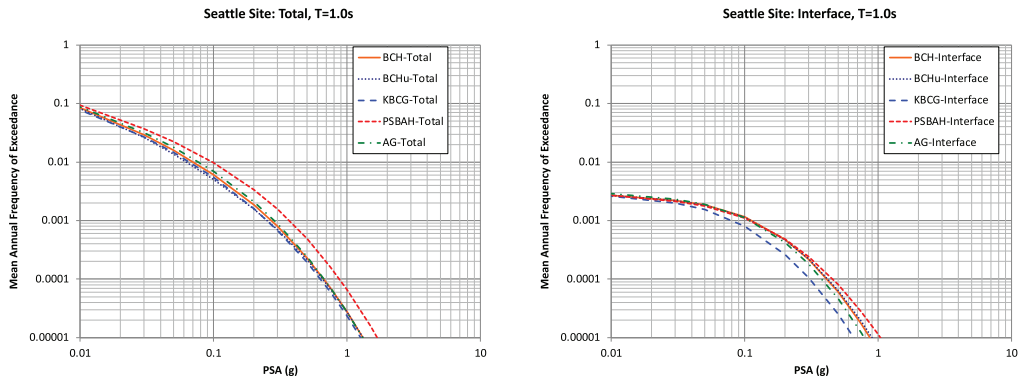
Figure 25. Comparison of total hazard curves separated by subduction GMM (left panel) and interface source hazard curve (right panel) for the Seattle site location for T = 1 sec.
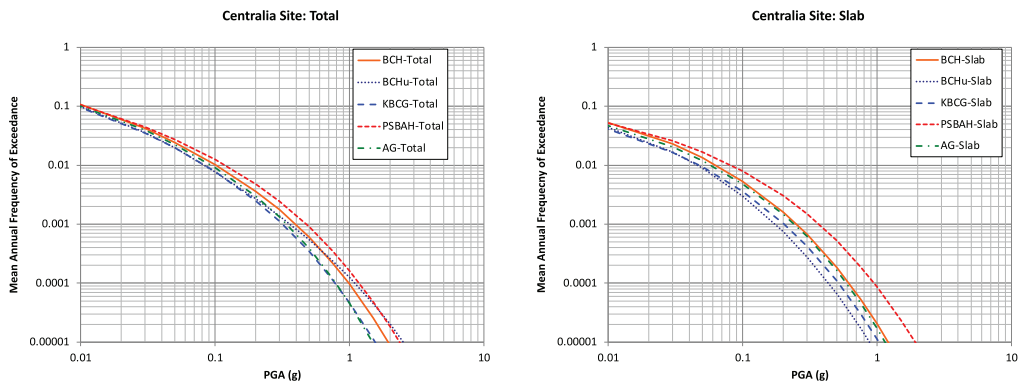

Figure 26. Comparison of total hazard curves separated by subduction GMM (left panel) and slab source hazard curve (right panel) for the Centralia site location for PGA.

Results for the Centralia site are presented in Figures 26 (PGA) and Figure 27 (T = 1 sec). Similar observations from the Seattle site results are noted for the Centralia site, with the ground motions from the PSBAH model being higher than the other models driven by the impact and contribution from the slab events. These relatively larger ground motions from the PSBAH model compared to the AG and KBCG models for the Cascadia regional versions are more significant at the $V_{S30} = 760$ m/sec value than for the 400 m/sec value (see the additional comparison provided in Supplemental Appendix A).

Based on the computed hazard curves, uniform hazard spectra ground motions are computed for return periods of 500 and 2475 years. For each case, the spectral ratio of the ground motions based on the individual GMMs with the BCH model being the reference model (i.e. denominator) is computed. The results are presented in Figure 28 for both the Seattle and Centralia sites. The overall impact for the AG and KBCG models is a slight reduction in the range of 0%-20% for these test cases. For the PSBAH model, the range in ground motion differences is larger, with variations as large as a 50% increase (T = 0.2 sec) to a 30% reduction (T = 5.0 sec). This observed impact for the shorter
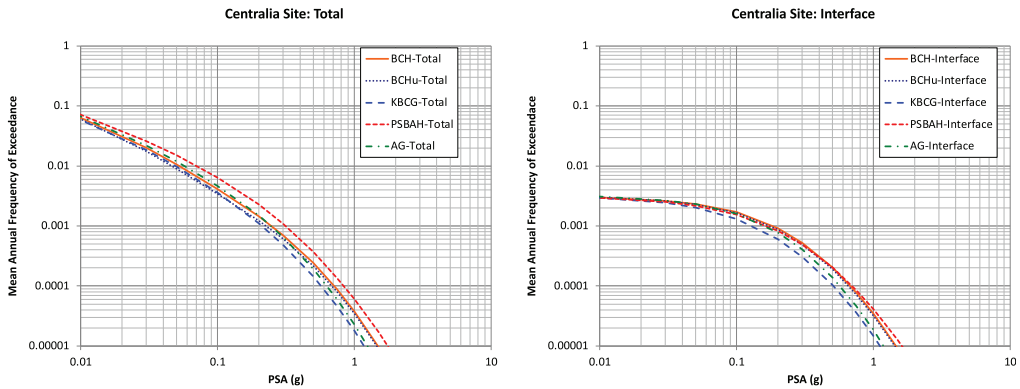
Figure 27. Comparison of total hazard curves separated by subduction GMM (left panel) and interface source hazard curve (right panel) for the Centralia site location for T = 1 sec.

spectral periods is based on the different regional site amplification scaling between the three NGA-Sub models for the V_{S30} = 760 m/sec case (e.g. see Figure 14 and the electronic files described in Supplemental Appendix A). Smaller differences are observed for the V_{S30} = 400 m/sec case, which would be expected to lead to lower differences in the uniform hazard spectrum (UHS) ratio values if computed.

Summary and conclusions

The development of the NGA-Sub database and the resulting NGA-Sub GMMs represents a significant improvement in the estimation of ground motions from subduction earthquakes. Limitations, however, still exist based on the sparse distribution of data from some of the subduction regions such as Cascadia. Even with this paucity of data for Cascadia, three of the models have regional adjustments for application to events in the Cascadia region. The development and justification for these adjustments are presented in the cited references for each of the GMMs. Similarly, three of the four currently developed NGA-Sub models have global and regionalized versions to allow for the application and adjustments of specific tectonic regions. The comparisons between these new NGA-Sub models for a given region or the global models indicate differences on the order of factors of 2 – 3 or less.

To assist with the understanding of these new models and their comparisons to previously published GMMs, this article shows various comparisons of the models. These selected scenario events are not meant to capture the full range of the models or their expected implementation, but rather to provide a small sample of representative scenario cases. Additional plots and the digital values for the attenuation curves and response spectra presented in this report are provided as part of the electronic supplement for this article (see Supplemental Appendix A).

Based on the observed variations in the PSHA calculations and any similar application to other regions and or projects, it is recommended that technically informed decisions based on the seismic hazard analysis being performed and the potential impacts of these new NGA-Sub GMMs should be completed prior to their implementation in a study. For specific applications, additional comparisons may and should be performed, allowing for
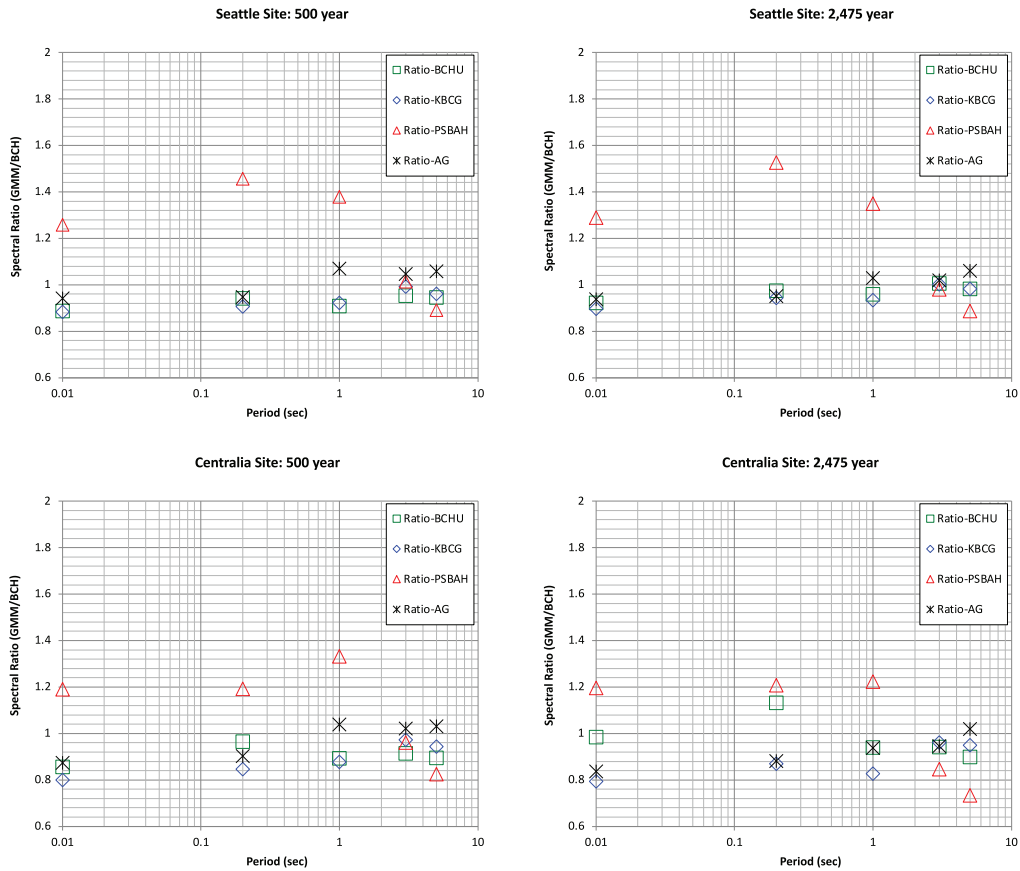
Figure 28. Spectral ratio of the UHS for the Seattle site for 500 year (upper left), 2475 year (upper right) and the Centralia site for 500 year (lower left) and 2475 year (lower right) hazard levels.

technical justifications for the implementation of these new models at the site of interest, including for the development of logic-tree weights.

Acknowledgments

Declaration of conflicting interests

The author(s) declared no potential conflicts of interest with respect to the research, authorship, and/ or publication of this article.

Funding

ORCID iDs

Nick Gregor https://orcid.org/0000-0002-7858-5403
Zeynep Gülerce https://orcid.org/0000-0003-4887-5415
Grace A Parker https://orcid.org/0000-0002-9445-2571
Hongjun Si https://orcid.org/0000-0002-3543-6029
Jonathan P Stewart https://orcid.org/0000-0003-3602-3629

Supplemental material

Supplemental material for this article is available online.

References

Abrahamson N and Gülerce Z (2020) *Ground-motion model for subduction zones based on the NGA-SUB data set*. PEER Report No. 2020/25. Berkeley, CA: Pacific Earthquake Engineering Research Center, University of California, Berkeley.

Abrahamson N and Gülerce Z (2021) Summary of the Abrahamson and Gulerce NGA-SUB ground-motion model for Subduction earthquakes. *Earthquake Spectra*.

Abrahamson N, Gregor N and Addo K (2016) BC hydro ground motion prediction equations for subduction earthquakes. *Earthquake Spectra* 32: 23–44.

Abrahamson N, Kuehn N, Gregor N, Bozorgnia Y, Parker GA, Stewart JP, Chiou B-SJ, Campbell KW and Youngs R (2018) *Update of the BC hydro Subduction ground-motion model using the NGA-Subduction dataset*. PEER Report No. 2018/02. Berkeley, CA: Pacific Earthquake Engineering Research Center, University of California, Berkeley.

Ahdi SK, Ancheta TD, Contreras V, Kishida T, Kwak DY, Kwok AOL, Parker GA, Ruz F and Stewart JP (2020) *Chapter 5: Site condition parameters, in data resources for NGA-Subduction Project*. PEER Report No. 2020/02. Berkeley, CA: Pacific Earthquake Engineering Research Center, University of California, Berkeley.

Ahdi SK, Kwak DY, Ancheta TD, Contreras V, Kishida T, Kwok AOL, Ruz F and Stewart JP (2021) NGA-sub site database. *Earthquake Spectra*.

Al Atik L, Abrahamson N, Bommer JJ, Scherbaum F, Cotton F and Kuehn N (2010) The variability of ground-motion prediction models and its components. *Seismological Research Letters* 81: 794–801.

Al Atik L and Youngs RR (2014) Epistemic uncertainty for NGA-West2 models. *Earthquake Spectra* 30: 1301–1318.

American Society of Civil Engineers (ASCE) (2017) *Minimum Desogn Loads and Associated Criteria for Buildings and Other Structures* (ASCE Standard 7-16). Reston, VA: American Society of Civil Engineers.

Atkinson GM and Boore DM (2003) Empirical ground-motion relationships for subduction-zone earthquakes and their application to Cascadia and other regions. *Bulletin of the Seismological Society of America* 93: 1703–1729.

Atkinson GM and Boore DM (2008) Erratum to empirical ground-motion relations for subduction zone earthquakes and their application to Cascadia and other regions. *Bulletin of the Seismological Society of America* 98: 2567–2569.

Atkinson GM and Macias M (2009) Predicted ground motions for great interface earthquakes in the Cascadia subduction zone. *Bulletin of the Seismological Society of America* 99: 1552–1578.

Boore DM and Kishida T (2017) Relations between some horizontal-component ground-motion intensity measured used in practice. *Bulletin of the Seismological Society of America* 107: 334–343.

Bozorgnia Y, Abrahamson NA, Ahdi SK, Ancheta TD, Al Atik L, Archuleta RJ, Atkinson GM, Boore DM, Campbell KW, Chiou BS-J, Contreras V, Darragh RB, Derakhshan S, Donahue JL, Gregor N, Gulerce Z, Idriss IM, Ji C, Kishida T, Kottke AR, Kuehn N, Kwak DY, Kwok AO-L, Lin P, Mazzoni S, Midorikawa S, Muin S, Parker GA, Rezaeian S, Si H, Silva WJ, Stewart JP, Walling M, Wooddell K and Youngs RR (2021) NGA-Subduction research program. *Earthquake Spectra*.

Bozorgnia Y, Abrahamson NA, Al Atik L, Ancheta TD, Atkinson GM, Baker JW, Baltay A, Boore DM, Campbell KW, Chiou BS-J, Darragh R, Day S, Donahue J, Graves RW, Gregor N, Hanks T, Idriss IM, Kamai R, Kishida T, Kottke A, Mahin SA, Rezaeian S, Rowshandel B, Seyhan E, Shahi S, Shantz T, Silva W, Spudich P, Stewart JP, Watson-Lamprey J, Wooddell K and Youngs R (2014) NGA-West2 research project. *Earthquake Spectra* 30: 973–987.

Bozorgnia Y and Stewart JP (2020) *Data resources for NGA-Subduction Project*. PEER No. Report 2020/02. Berkeley, CA: Pacific Earthquake Engineering Research Center, University of California, Berkeley.

Building Seismic Safety Council (2009) NEHRP recommended seismic provisions for new buildings and other structures (FEMA Report P-750). Available at: http://www.fema.gov/media-library/ assets/documents/18152?id = 4103 Last accessed 19 January 2021.

Campbell KW (2020) Proposed methodology for estimating the magnitude at which subduction megathrust ground motions and source dimensions exhibit a break in magnitude scaling: Example for 79 global subduction zones. *Earthquake Spectra* 36: 1271–1297.

Contreras V, Stewart JP, Kishida T, Darragh RB, Chiou BS-J, Mazzoni S, Kuehn N, Ahdi SK, Wooddell K, Youngs RR, Bozorgnia Y, Boroschek R, Rojas F and Órdenes J (2020) *Chapter 4: Source and Path Metadata* (ed JP Stewart, PEER Report No. 2020/02). Berkeley, CA: Pacific Earthquake Engineering Research Center, University of California, Berkeley.

Contreras V, Stewart JP, Kishida T, Darragh RB, Chiou BS-J, Mazzoni S, Youngs RR, Kuehn N, Ahdi SK, Boroschek R, Rojas F and Órdenes J (2021) NGA-sub source and path database. *Earthquake Spectra*.

Gregor N, Abrahamson NA, Atkinson GM, Boore DM, Bozorgnia Y, Campbell KW, Chiou BS-J, Idriss IM, Kamai R, Seyhan E, Silva WJ, Stewart JP and Youngs RR (2014) Comparison of NGA-West2 GMPEs. *Earthquake Spectra* 30: 1179–1197.

Gregor N, Addo K, Al Atik L, Atkinson G, Boore D, Bozorgnia Y, Campbell K, Chiou B, Gülerce Z, Hassani B, Kishida T, Kuehn N, Midorijawa S, Mazzoni S, Parker G, Si H, Stewart JP and Youngs R (2020) *Comparison of NGA-sub ground motion models*. PEER Report 2020/07. Berkeley, CA: Pacific Earthquake Engineering Research Center, University of California, Berkeley.

Gregor N, Silva W, Wong I and Youngs R (2002) Ground-motion attenuation relationships for Cascadia subduction zone megathrust earthquakes based on a stochastic finite-fault modeling. *Bulletin of the Seismological Society of America* 92: 1923–1932.

Ji C and Archuleta RJ (2018) *Scaling of PGA and PGV Deduced from Numerical Simulations of Intraslab Earthquakes*. Santa Barbara, CA: Department of Earth Science, University of California, Santa Barbara.

Kishida T, Darragh RB, Chiou BS-J, Bozorgnia Y, Mazzoni S, Contreras V, Boroschek R, Rojas F and Stewart JP (2020) *Chapter 3: Ground Motions and Intensity Measures, in Data Resources for*

NGA-Subduction Project (ed JP Stewart, PEER Report 2020/02). Berkeley, CA: Pacific Earthquake Engineering Research Center, University of California, Berkeley.

Kuehn N, Bozorgnia Y, Campbell KW and Gregor N (2020) *Partially nonergodic ground-motion model for subduction regions using NGA-Subduction database*. PEER Report No. 2020/04. Berkeley, CA: Pacific Earthquake Engineering Research Center, University of California, Berkeley.

Kuehn N, Bozorgnia Y, Campbell KW and Gregor N (2021) Partially non-ergodic ground-motion model for subduction regions using NGA-Subduction database. *Earthquake Spectra*.

McGuire RK (2004) *Seismic Hazard and Risk Analysis* (EERI Monograph MNO-10). Oakland, CA: Earthquake Engineering Research Institute.

Mazzoni S, Kishida T, Stewart JP, Darragh RB, Ancheta TA, Chiou BS-J, Silva WJ and Bozorgnia Y (2021) NGA-Sub relational database. *Earthquake Spectra*.

Parker GA, Stewart JP, Boore DM, Atkinson GM and Hassani B (2020) *NGA-Subduction global ground-motion model with regional adjustment factors*. PEER Report No. 2020/03. Berkeley, CA: Pacific Earthquake Engineering Research Center, University of California, Berkeley.

Parker GA, Stewart JP, Boore DM, Atkinson GM and Hassani B (2021) NGA-Subduction global ground motion models with regional adjustment factors. *Earthquake Spectra*.

Petersen MD, Moshetti MP, Powers PM, Mueller CS, Haller KM, Frankel AD, Zeng Y, Rezaeian S, Harmsen SC, Boyd OS, Field EH, Chen R, Rukstales KS, Luco N, Wheeler RL, Williams RA and Olsen AH (2014) *Documentation for the 2014 update of the United States National Seismic Hazard Maps*. USGS Open File Report 2014-1091. Reston, VA: United States Geological Survey.

Petersen MD, Shumway AM, Powers PM, Mueller CS, Moschetti MP, Frankel AD, Rezaeian S, McNamara DE, Luco N, Boyd OS, Rukstales KS, Hoover SM, Clayton BS, Field EH and Zang Y (2020) The 2018 update of the US National Seismic Hazard Model: Overview of model and implications. *Earthquake Spectra* 36: 5–41.

Si H, Midorikawa S and Kishida T (2020) *Development of NGA-sub ground-motion model of 5%-damped pseudo-spectral acceleration based on database for subduction earthquakes in Japan*. PEER Report. Berkeley, CA: Pacific Earthquake Engineering Research Center, University of California, Berkeley (center headquarters).

Zhao JX, Jiang F, Shi P, Xing H, Huang H, Hou R, Zhang Y, Yu P, Lan X, Rhoades DA and Somerville PG (2016a) Ground-motion prediction equations for subduction slab earthquakes in Japan using site class and simple geometric attenuation functions. *Bulletin of the Seismological Society of America* 106: 1535–1551.

Zhao JX, Liang X, Jiang F, Xing H, Zhu M, Hou R, Zhang Y, Lan X, Rhoades DA, Irikura K and Fukushima Y (2016b) Ground-motion prediction equations for subduction interface earthquakes in Japan using site class and simple geometric attenuation functions. *Bulletin of the Seismological Society of America* 106: 1518–1534.

Zhao JX, Zhang J, Asano A, Ohno Y, Oouchi T, Takahashi T, Ogawa H, Irikura K, Thio HK, Somerville PG, Fukushima Y and Fukushima Y (2006) Attenuation relations of strong ground motion in Japan using site classification based on predominant period. *Bulletin of the Seismological Society of America* 96: 898–913.